Atmospheric Chemistry Suite:
Science Overview

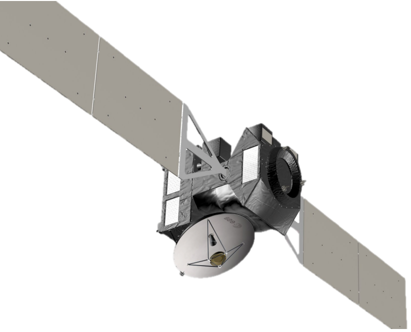

f. montme Cliquez

LATMOS CNRS, Franc

ACS Science Team M
Moscow,

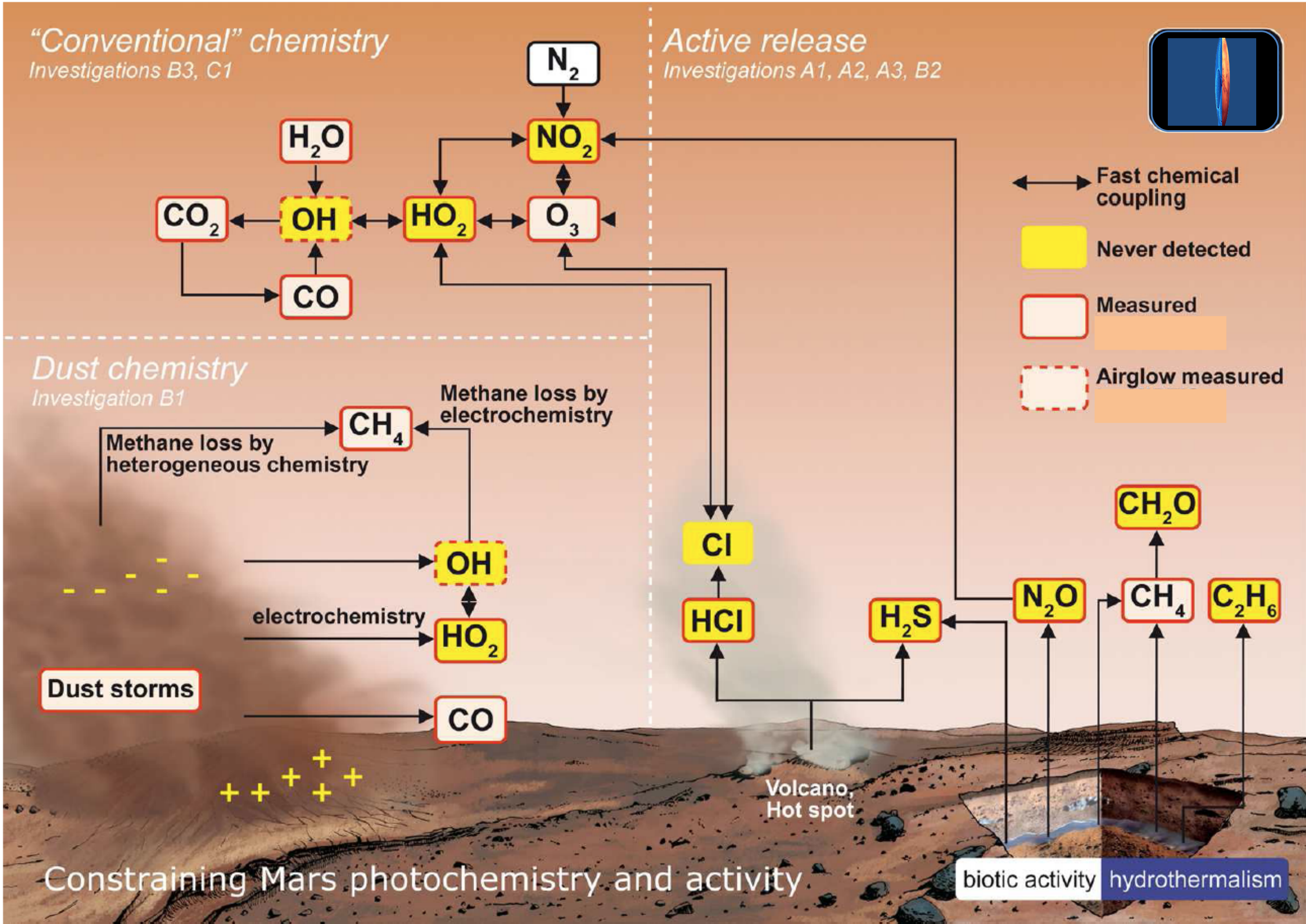

2016

TECHNOLOGY OBJECTIVE

- Entry, Descent, and Landing (EDL) of a payload on the surface of Mars.

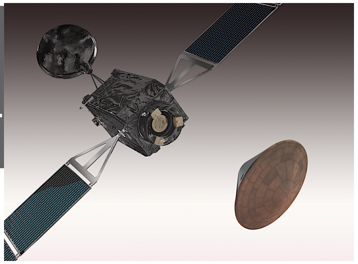

SCIENTIFIC OBJECTIVE

- To study Martian atmospheric trace gases and their sources, **possibie signature of geophysical or biological activity.**

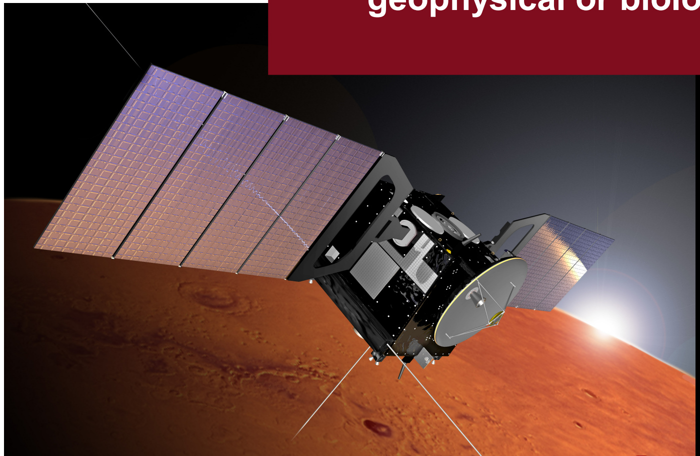

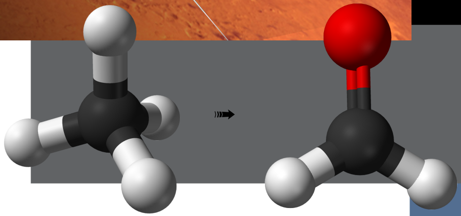

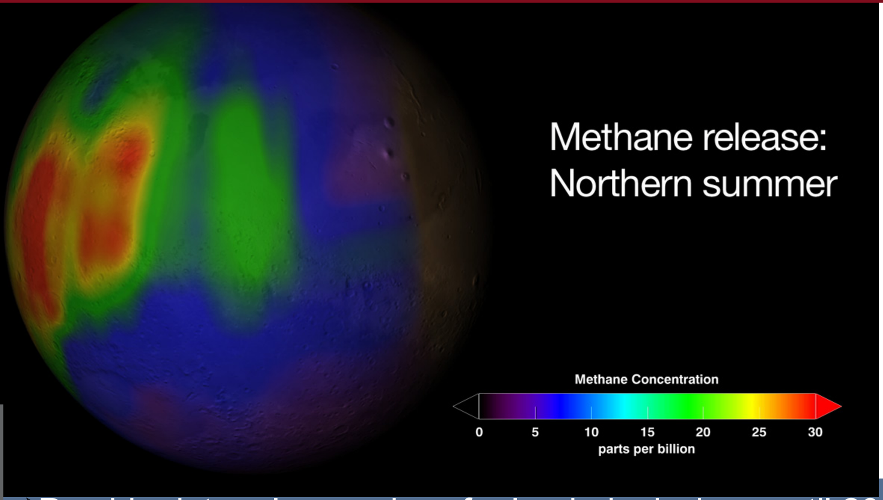

- Provide data relay services for landed missions until 2022.

ExoMars Scientific Objectives

- To search for signs of past and present life on Mars
- To investigate the water/geochemical environment as a function of depth in the shallow subsurface
- To investigate Martian atmospheric trace gases and their sources.

Trace Gas Orbiter Objectives

- Detection of a broad suite of atmospheric trace gases, **possible signature of geophysical/biological activity on Mars**
- Characterization of their spatial and temporal variation
- Localization of the sources of key trace gases

What geophysical gases should we expect?

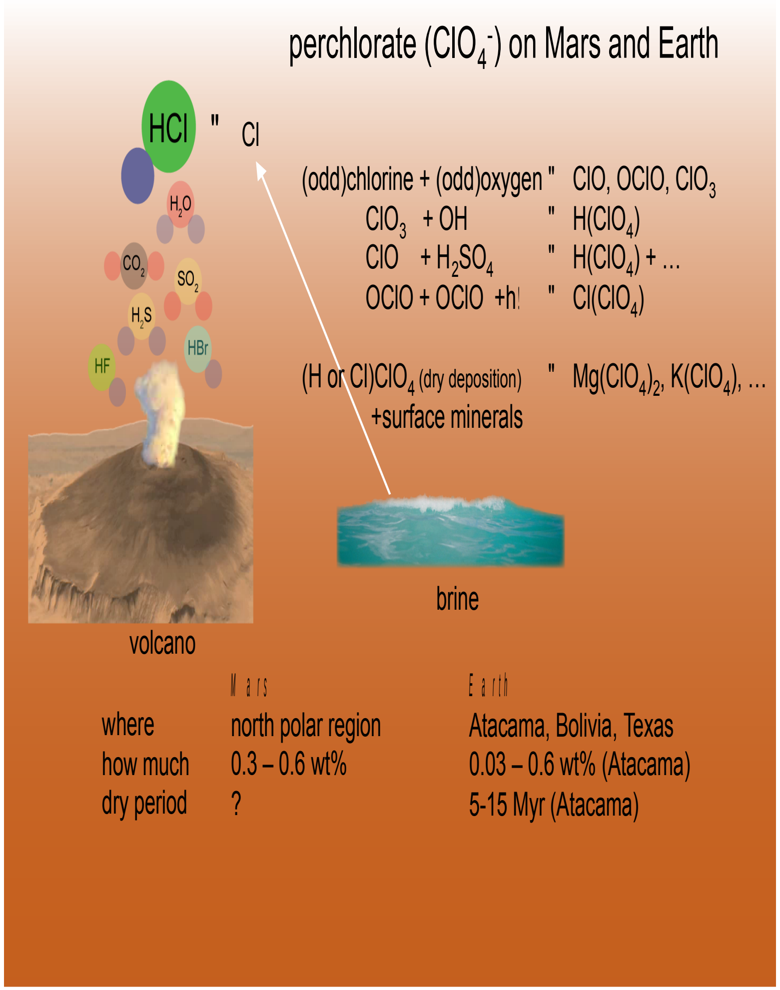

perchlorate (ClO_4^-) on Mars and Earth

HCl " Cl

(odd)chlorine + (odd)oxygen " ClO, OClO, ClO_3
ClO_3 + OH " $H(ClO_4)$
ClO + H_2SO_4 " $H(ClO_4)$ + ...
OClO + OClO +h! " $Cl(ClO_4)$

(H or Cl)ClO_4 (dry deposition) " $Mg(ClO_4)_2$, $K(ClO_4)$, ...
+surface minerals

	Mars	Earth
where	north polar region	Atacama, Bolivia, Texas
how much	0.3 – 0.6 wt%	0.03 – 0.6 wt% (Atacama)
dry period	?	5-15 Myr (Atacama)

On the Earth, the principal components of volcanic gases are water vapor (**H2O**), carbon dioxide (**CO2**), sulfur either as sulfur dioxide (**SO2**) (high-temperature volcanic gases) or hydrogen sulfide (**H2S**) (low-temperature volcanic

List of TGO high priority target species

H2O, HO2, H2O2, NO2, N2O, CH4, C2H2, C2H4, C2H6, H2CO, HCN, H2S, OCS, SO2, HCl, CO, O3

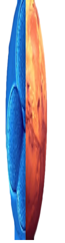

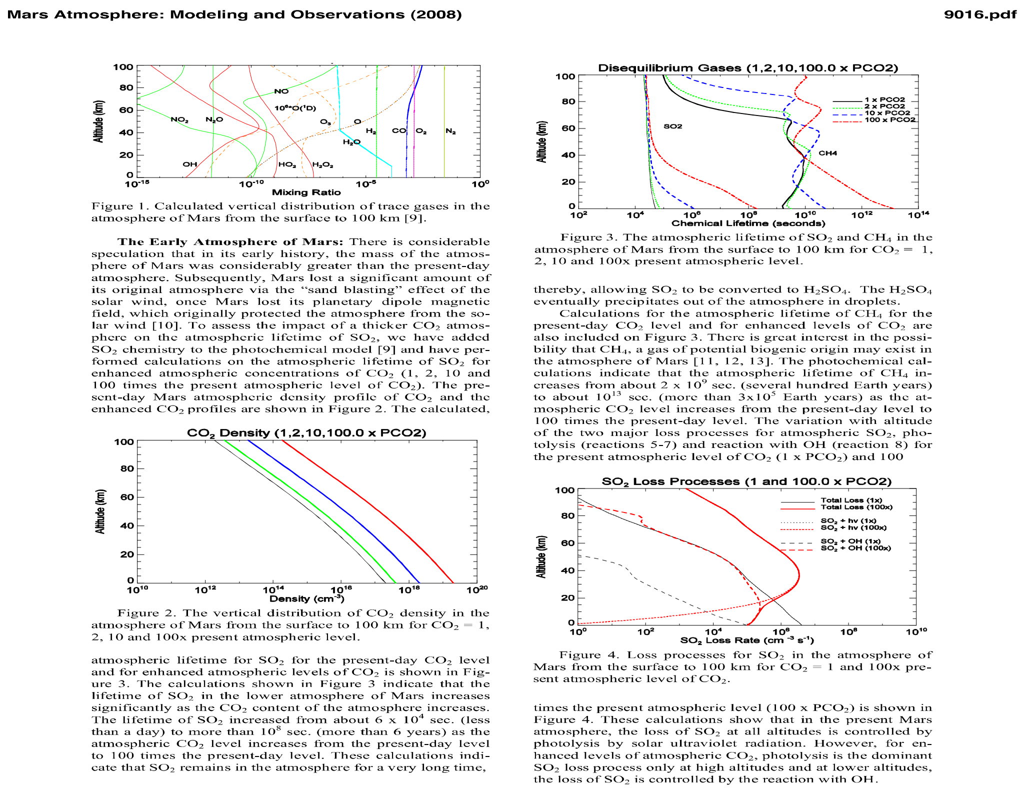
Mars Atmosphere: Modeling and Observations (2008)

9016.pdf

Figure 1. Calculated vertical distribution of trace gases in the atmosphere of Mars from the surface to 100 km [9].

The Early Atmosphere of Mars: There is considerable speculation that in its early history, the mass of the atmosphere of Mars was considerably greater than the present-day atmosphere. Subsequently, Mars lost a significant amount of its original atmosphere via the "sand blasting" effect of the solar wind, once Mars lost its planetary dipole magnetic field, which originally protected the atmosphere from the solar wind [10]. To assess the impact of a thicker CO_2 atmosphere on the atmospheric lifetime of SO_2, we have added SO_2 chemistry to the photochemical model [9] and have performed calculations on the atmospheric lifetime of SO_2 for enhanced atmospheric concentrations of CO_2 (1, 2, 10 and 100 times the present atmospheric level of CO_2). The present-day Mars atmospheric density profile of CO_2 and the enhanced CO_2 profiles are shown in Figure 2. The calculated, atmospheric lifetime for SO_2 for the present-day CO_2 level and for enhanced atmospheric levels of CO_2 is shown in Figure 3. The calculations shown in Figure 3 indicate that the lifetime of SO_2 in the lower atmosphere of Mars increases significantly as the CO_2 content of the atmosphere increases. The lifetime of SO_2 increased from about 6 x 10^4 sec. (less than a day) to more than 10^8 sec. (more than 6 years) as the atmospheric CO_2 level increases from the present-day level to 100 times the present-day level. These calculations indicate that SO_2 remains in the atmosphere for a very long time, thereby, allowing SO_2 to be converted to H_2SO_4. The H_2SO_4 eventually precipitates out of the atmosphere in droplets.

Figure 2. The vertical distribution of CO_2 density in the atmosphere of Mars from the surface to 100 km for CO_2 = 1, 2, 10 and 100x present atmospheric level.

Calculations for the atmospheric lifetime of CH_4 for the present-day CO_2 level and for enhanced levels of CO_2 are also included on Figure 3. There is great interest in the possibility that CH_4, a gas of potential biogenic origin may exist in the atmosphere of Mars [11, 12, 13]. The photochemical calculations indicate that the atmospheric lifetime of CH_4 increases from about 2 x 10^9 sec. (several hundred Earth years) to about 10^{13} sec. (more than 3x10^5 Earth years) as the atmospheric CO_2 level increases from the present-day level to 100 times the present-day level. The variation with altitude of the two major loss processes for atmospheric SO_2, photolysis (reactions 5-7) and reaction with OH (reaction 8) for the present atmospheric level of CO_2 (1 x PCO_2) and 100 times the present atmospheric level (100 x PCO_2) is shown in Figure 4. These calculations show that in the present Mars atmosphere, the loss of SO_2 at all altitudes is controlled by photolysis by solar ultraviolet radiation. However, for enhanced levels of atmospheric CO_2, photolysis is the dominant SO_2 loss process only at high altitudes and at lower altitudes, the loss of SO_2 is controlled by the reaction with OH.

Figure 3. The atmospheric lifetime of SO_2 and CH_4 in the atmosphere of Mars from the surface to 100 km for CO_2 = 1, 2, 10 and 100x present atmospheric level.

Figure 4. Loss processes for SO_2 in the atmosphere of Mars from the surface to 100 km for CO_2 = 1 and 100x present atmospheric level of CO_2.

- Most chemical species released by geophysical activity have "short" chemical lifetimes:
  - CH4 300 yrs
  - SO2 1-2 years
  - CO 3 years
- While CO2 and H2O already exist in significant quantities (detecting fluctuations is difficult and ambiguous wrt. other potential processes)
- The search for geochemical gases can only trace very recent or ongoing activities

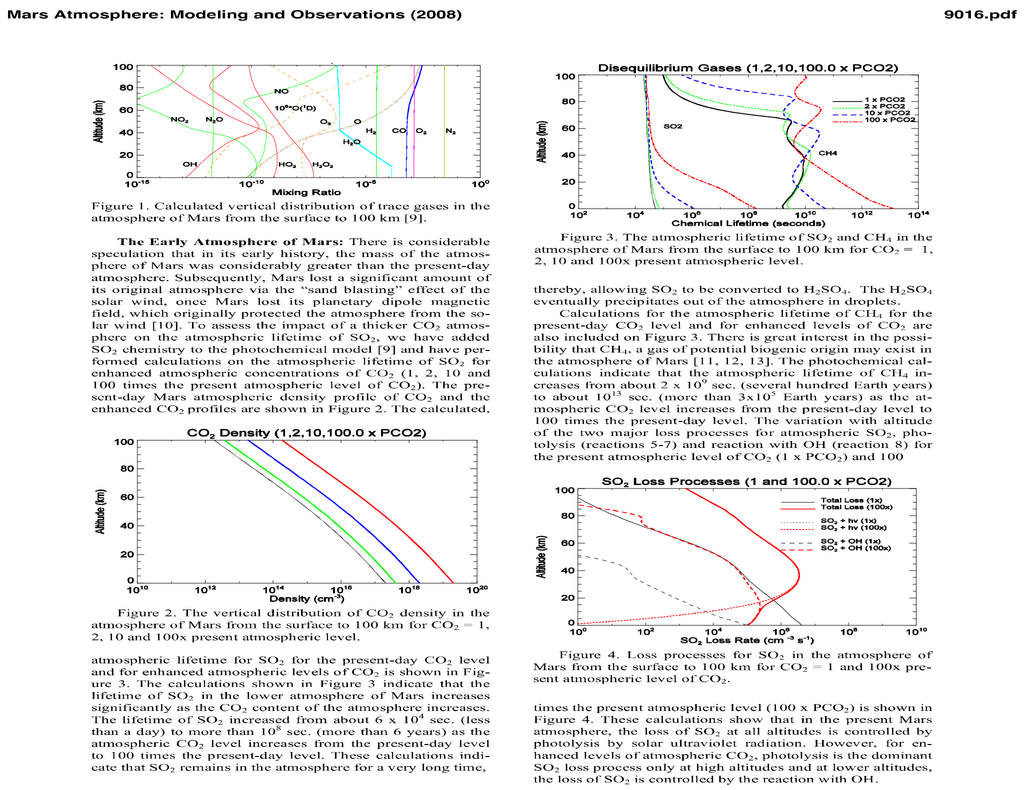

Mars Atmosphere: Modeling and Observations (2008) 9016.pdf

Figure 1. Calculated vertical distribution of trace gases in the atmosphere of Mars from the surface to 100 km [9].

The Early Atmosphere of Mars: There is considerable speculation that in its early history, the mass of the atmosphere of Mars was considerably greater than the present-day atmosphere. Subsequently, Mars lost a significant amount of its original atmosphere via the "sand blasting" effect of the solar wind, once Mars lost its planetary dipole magnetic field, which originally protected the atmosphere from the solar wind [10]. To assess the impact of a thicker CO_2 atmosphere on the atmospheric lifetime of SO_2, we have added SO_2 chemistry to the photochemical model [9] and have performed calculations on the atmospheric lifetime of SO_2 for enhanced atmospheric concentrations of CO_2 (1, 2, 10 and 100 times the present atmospheric level of CO_2). The present-day Mars atmospheric density profile of CO_2 and the enhanced CO_2 profiles are shown in Figure 2. The calculated,

Figure 2. The vertical distribution of CO_2 density in the atmosphere of Mars from the surface to 100 km for CO_2 = 1, 2, 10 and 100x present atmospheric level.

atmospheric lifetime for SO_2 for the present-day CO_2 level and for enhanced atmospheric levels of CO_2 is shown in Figure 3. The calculations shown in Figure 3 indicate that the lifetime of SO_2 in the lower atmosphere of Mars increases significantly as the CO_2 content of the atmosphere increases. The lifetime of SO_2 increased from about 6 x 10^4 sec. (less than a day) to more than 10^8 sec. (more than 6 years) as the atmospheric CO_2 level increases from the present-day level to 100 times the present-day level. These calculations indicate that SO_2 remains in the atmosphere for a very long time,

Figure 3. The atmospheric lifetime of SO_2 and CH_4 in the atmosphere of Mars from the surface to 100 km for CO_2 = 1, 2, 10 and 100x present atmospheric level.

thereby, allowing SO_2 to be converted to H_2SO_4. The H_2SO_4 eventually precipitates out of the atmosphere in droplets.

Calculations for the atmospheric lifetime of CH_4 for the present-day CO_2 level and for enhanced levels of CO_2 are also included on Figure 3. There is great interest in the possibility that CH_4, a gas of potential biogenic origin may exist in the atmosphere of Mars [11, 12, 13]. The photochemical calculations indicate that the atmospheric lifetime of CH_4 increases from about 2 x 10^9 sec. (several hundred Earth years) to about 10^{13} sec. (more than 3x10^5 Earth years) as the atmospheric CO_2 level increases from the present-day level to 100 times the present-day level. The variation with altitude of the two major loss processes for atmospheric SO_2, photolysis (reactions 5-7) and reaction with OH (reaction 8) for the present atmospheric level of CO_2 (1 x PCO_2) and 100

Figure 4. Loss processes for SO_2 in the atmosphere of Mars from the surface to 100 km for CO_2 = 1 and 100x present atmospheric level of CO_2.

times the present atmospheric level (100 x PCO_2) is shown in Figure 4. These calculations show that in the present Mars atmosphere, the loss of SO_2 at all altitudes is controlled by photolysis by solar ultraviolet radiation. However, for enhanced levels of atmospheric CO_2, photolysis is the dominant SO_2 loss process only at high altitudes and at lower altitudes, the loss of SO_2 is controlled by the reaction with OH.

- Most chemical species released by geophysical activity have "short" chemical lifetimes:
  - CH4 300 yrs
  - SO2 1-2 years
  - CO 3 years

- While CO2 and H2O already exist in significant quantities (detecting fluctuations is difficult and ambiguous wrt. other potential processes)

- The search for geochemical gases can only trace very recent or ongoing activities

Is there surface hints of current/recent geophysical activity on Mars?

- Geomorphological evidences of recent volcanic activity (106-7 yrs)
- Sulfate deposits in the North polar region (Langevin et al., 2005; Fishbaugh et al., 2007)
- However, Themis IR mapper sees no hot spot (Christensen, 2003)

Is there surface hints of current/recent geophysical activity on Mars?

- Geomorphological evidences of recent volcanic activity (106-7 yrs)
- Sulfate deposits in the North polar region (Langevin et al., 2005; Fishbaugh et al., 2007)
- Themis IR mapper sees no hot spot (Christensen, 2003)

TGO science instruments

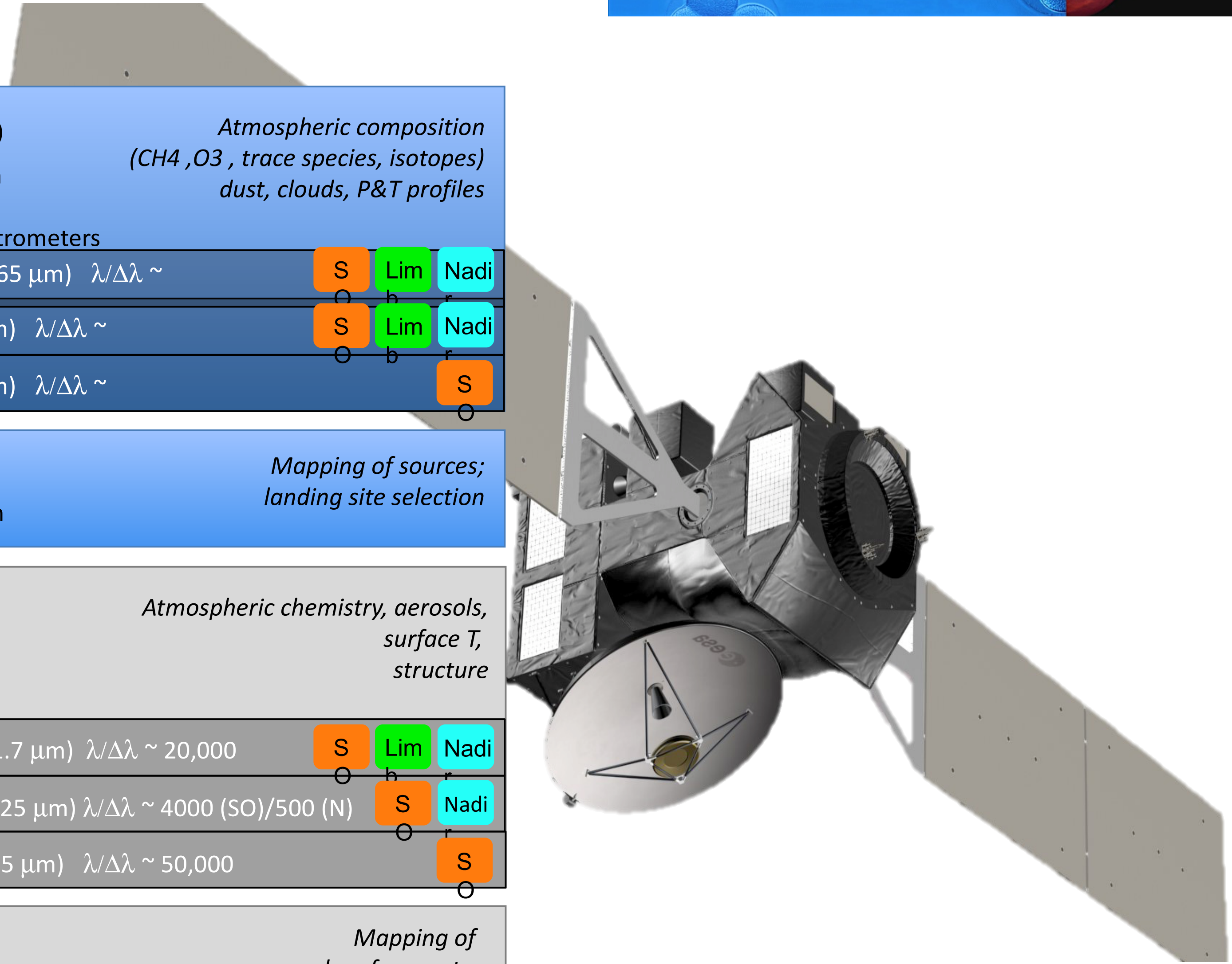

NOMAD

High resolution occultation and nadir spectrometers

Atmospheric composition (CH4 ,O3 , trace species, isotopes) dust, clouds, P&T profiles

UVIS (0.20 – 0.65 µm) λ/Δλ ~ 250	SO	Limb	Nadir
IR (2.3 – 3.8 µm) λ/Δλ ~ 10,000	SO	Limb	Nadir
IR (2.3 – 4.3 µm) λ/Δλ ~			SO

CaSSIS

High-resolution camera

Mapping of sources; landing site selection

ACS

Suite of 3 high-resolution spectrometers

Atmospheric chemistry, aerosols, surface T, structure

Near IR (0.7 – 1.7 µm) λ/Δλ ~ 20,000	SO	Limb	Nadir
IR (Fourier, 2 – 25 µm) λ/Δλ ~ 4000 (SO)/500 (N)		SO	Nadir
Mid IR (2.2 – 4.5 µm) λ/Δλ ~ 50,000			SO

FREND

Collimated neutron detector

Mapping of subsurface water

All resolving power figures λ/Δλ are calculated at mid-range

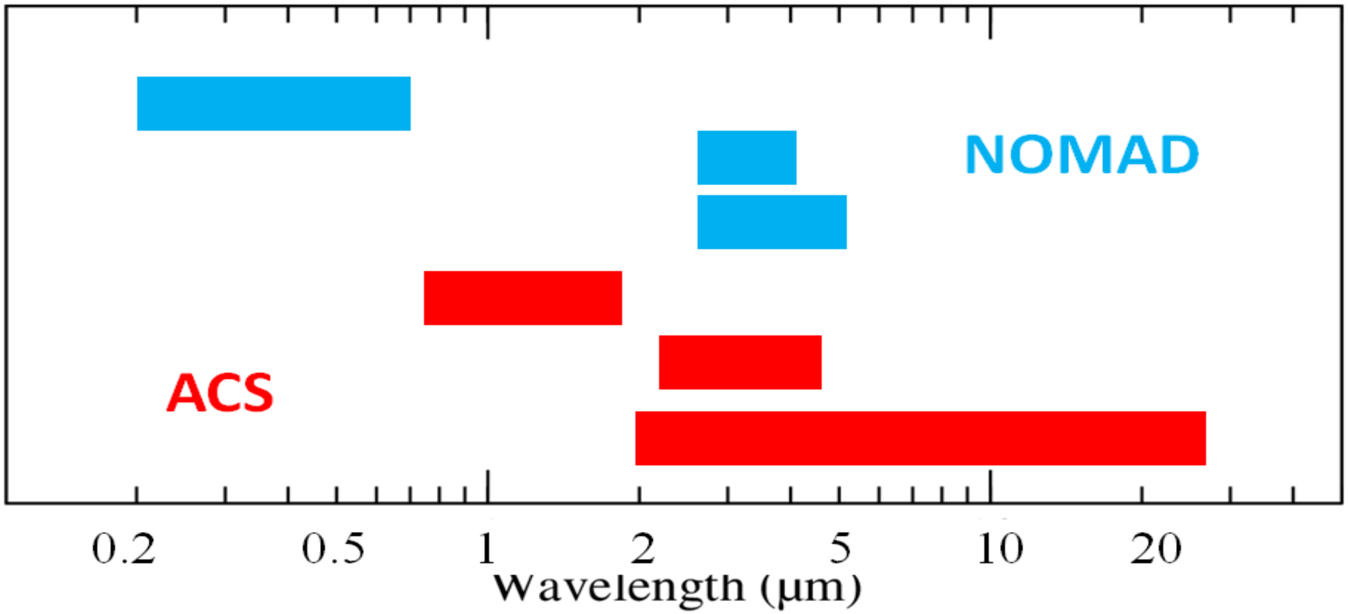

The ACS-NOMAD Complementarity

ACS: Major Science themes

- “Breakthrough” Science
  - with MIR channel Solar Occultations
  - **Trace Gas detection** with ppt sensitivity or/and **revisit upper limits**
    (may probably set an “all time” reference for future exploration missions)
- “Novel” Science
  - with all channels in Nadir/Occultation
  - **First mapping of D/H ratio**
    new information on water reservoirs and their history, cloud processes
  - **Oxidant species**
    HOx family (*e.g.* H2O2, OH, HO2) barely characterized on Mars, only reactants (O3)
- “Climatological” Science
  - with TIRVIM and Near-IR in nadir
  - **Mapping of meteorological fields**
    temperature, dust / ice aerosols, water vapor

O3, SO2,
*NO

H2O,
*O2, *OH, *NO

CH4, H2O, HO2,
HDO, HF, HCL,
SO2 CO2 +
isotopes, etc.

CO2, H2O2
dust, water ice

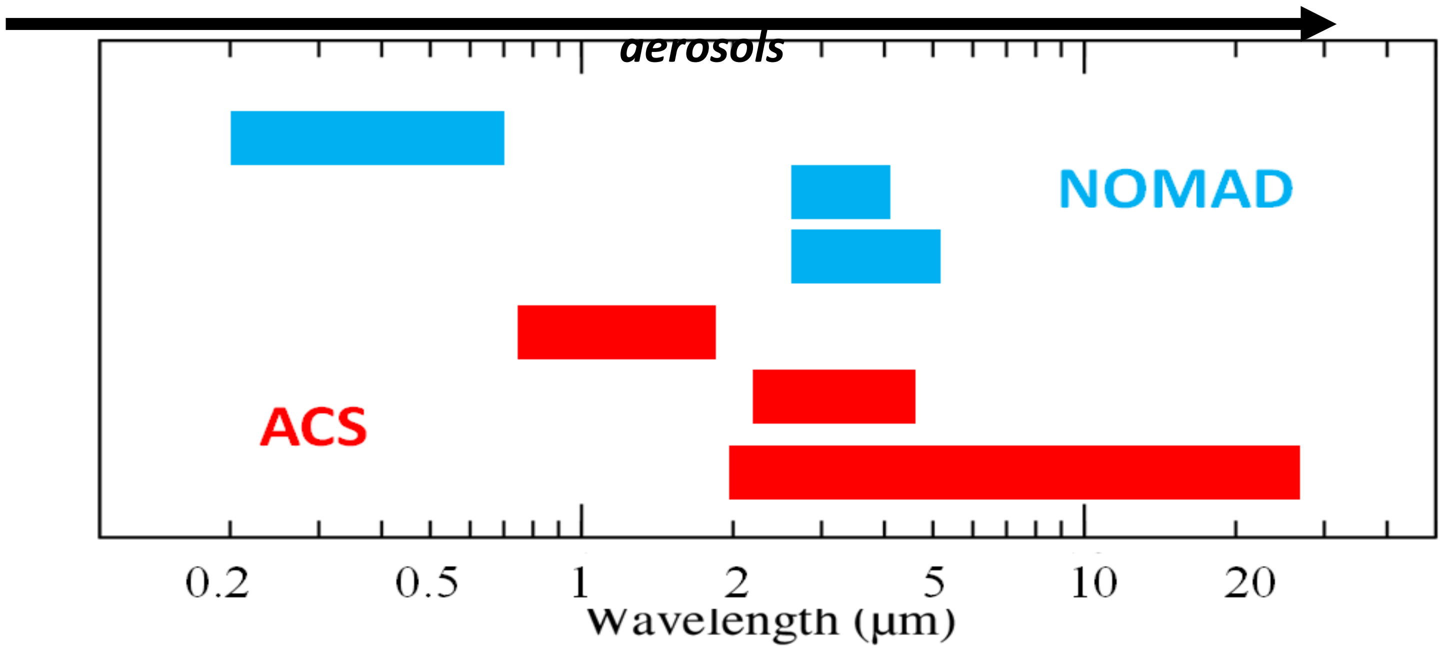

The ACS-NOMAD Complementarity

ACS-NOMAD:
synchronizing the approaches?

- Two comparable and highly capable instruments on the same platform
- This mission may set a new standard for Mars atmosphere composition. For this reason, it is probably better to have one single and loud voice
- Complementarity (spectral and thus scientific) between the two instruments is obvious: may lead to common effort threads (oxidants + O3)
- ExoMars TGO will feel the pressure of a community expecting confirmation/contradiction of CH4 existence
- Two instruments saying the same thing at the same time is the safest way to go to make results believable by our community
- Corrdinate announcement for (non)detection of any “hot” trace gas species (by the ExoMars Project Scientist)
- Scientific coordination between the two instruments should be a major task of ExoMars Project

Suggestions for Science Management Plan for ACS

- Having data pipeline ready by Mars Orbit Insertion will be critical for a prompt delivery of early results (upper limits or detection of trace species)
- We should define a priority ordering and a elaborate a schedule for **building and testing data pipelines** (example of MAVEN: data pipeline ready at launch, counter-example of SPICAM-UV: pipeline insufficiently mature, first conclusion proved to be wrong)

Trace species visible in the IR

“Hydrocarbons window” (CH4, C2H6, CH3OH, C2H4, etc.)

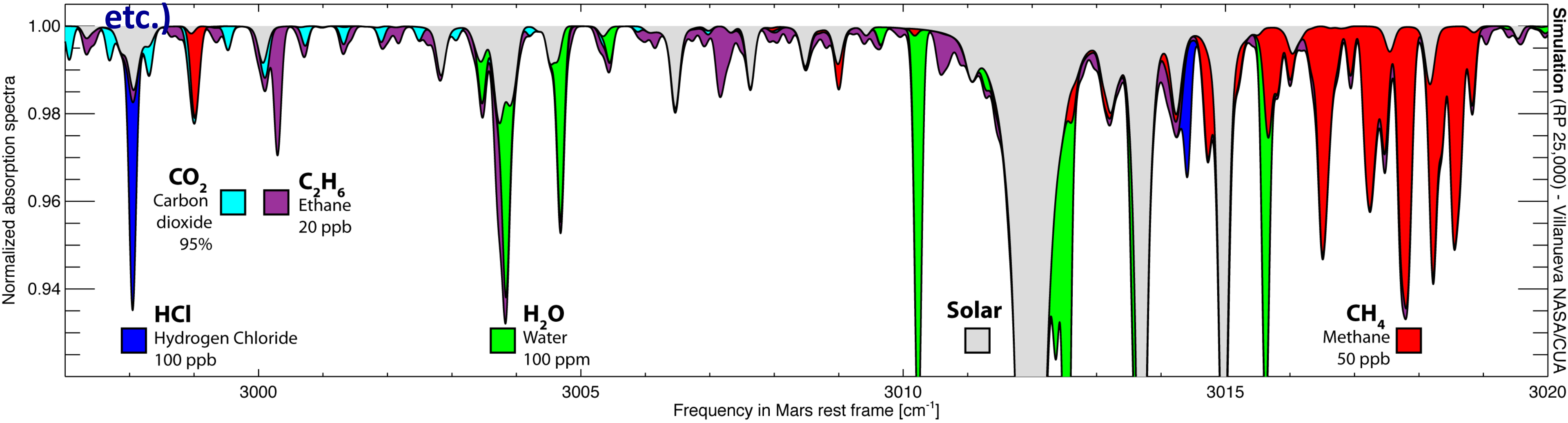

“Water D/H window”

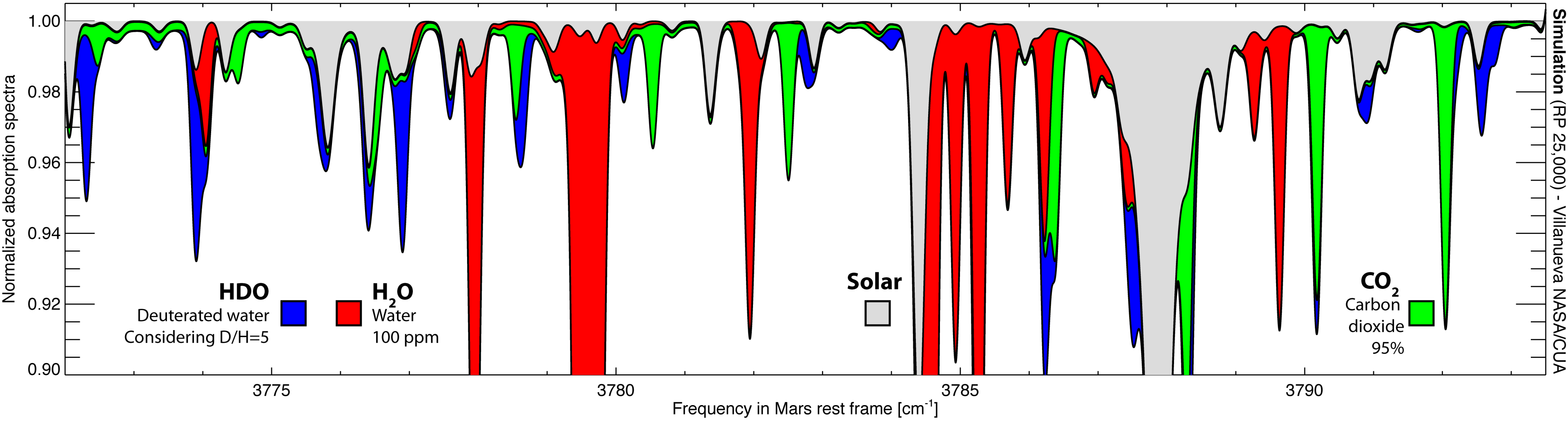

ACS observations in Solar Occultations

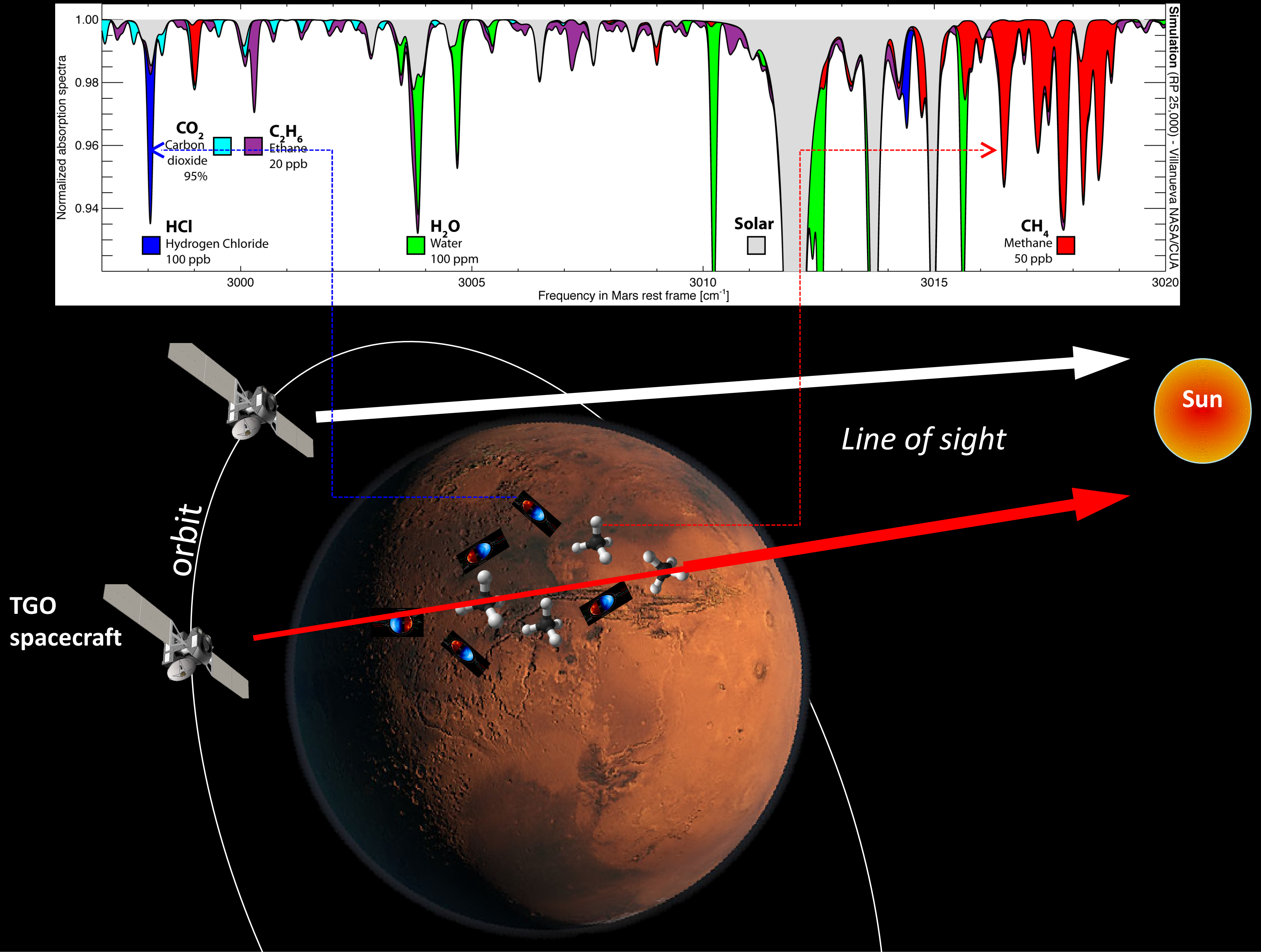

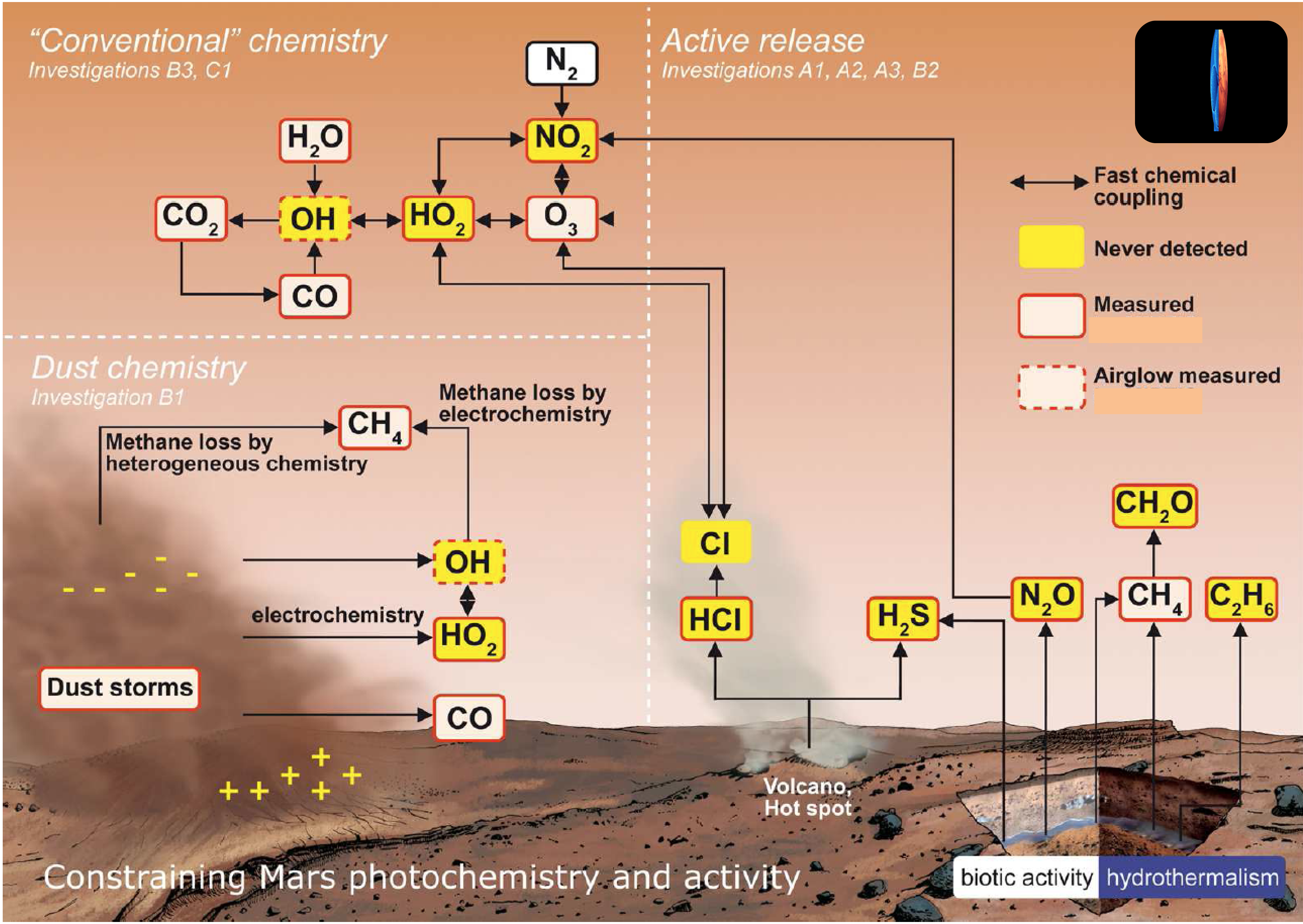

"Conventional" chemistry

Investigations B3, C1

N_2

H_2O

NO_2

CO_2

OH

HO_2

O_3

CO

Active release

Investigations A1, A2, A3, B2

↔ Fast chemical coupling

🟨 Never detected

Measured

Airglow measured

Dust chemistry

Investigation B1

CH_4

Methane loss by electrochemistry

Methane loss by heterogeneous chemistry

OH

electrochemistry

HO_2

Dust storms

CO

Cl

HCl

H_2S

Volcano, Hot spot

CH_2O

N_2O

CH_4

C_2H_6

biotic activity

hydrothermalism

Constraining Mars photochemistry and activity

Convential (known) chemistry

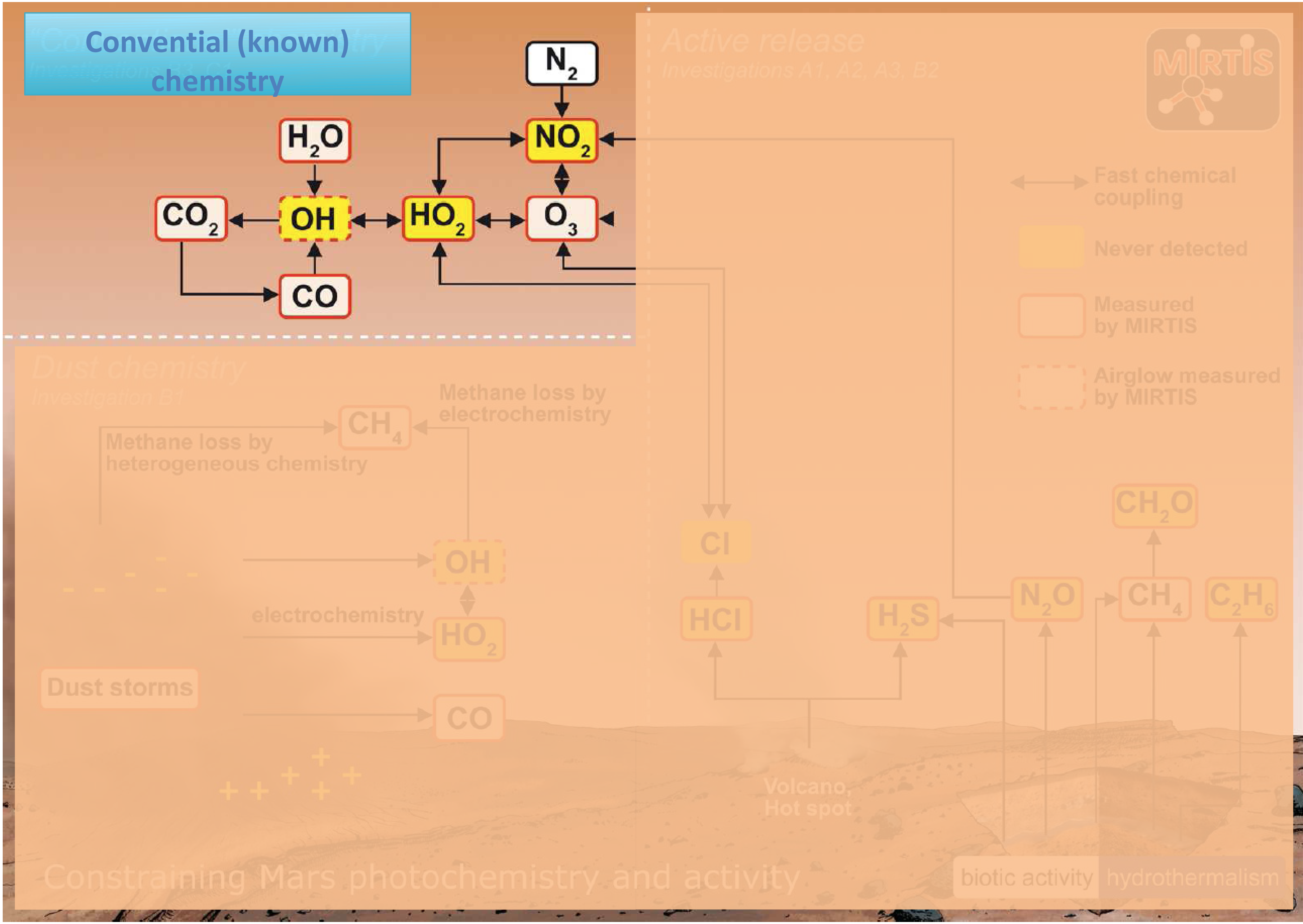

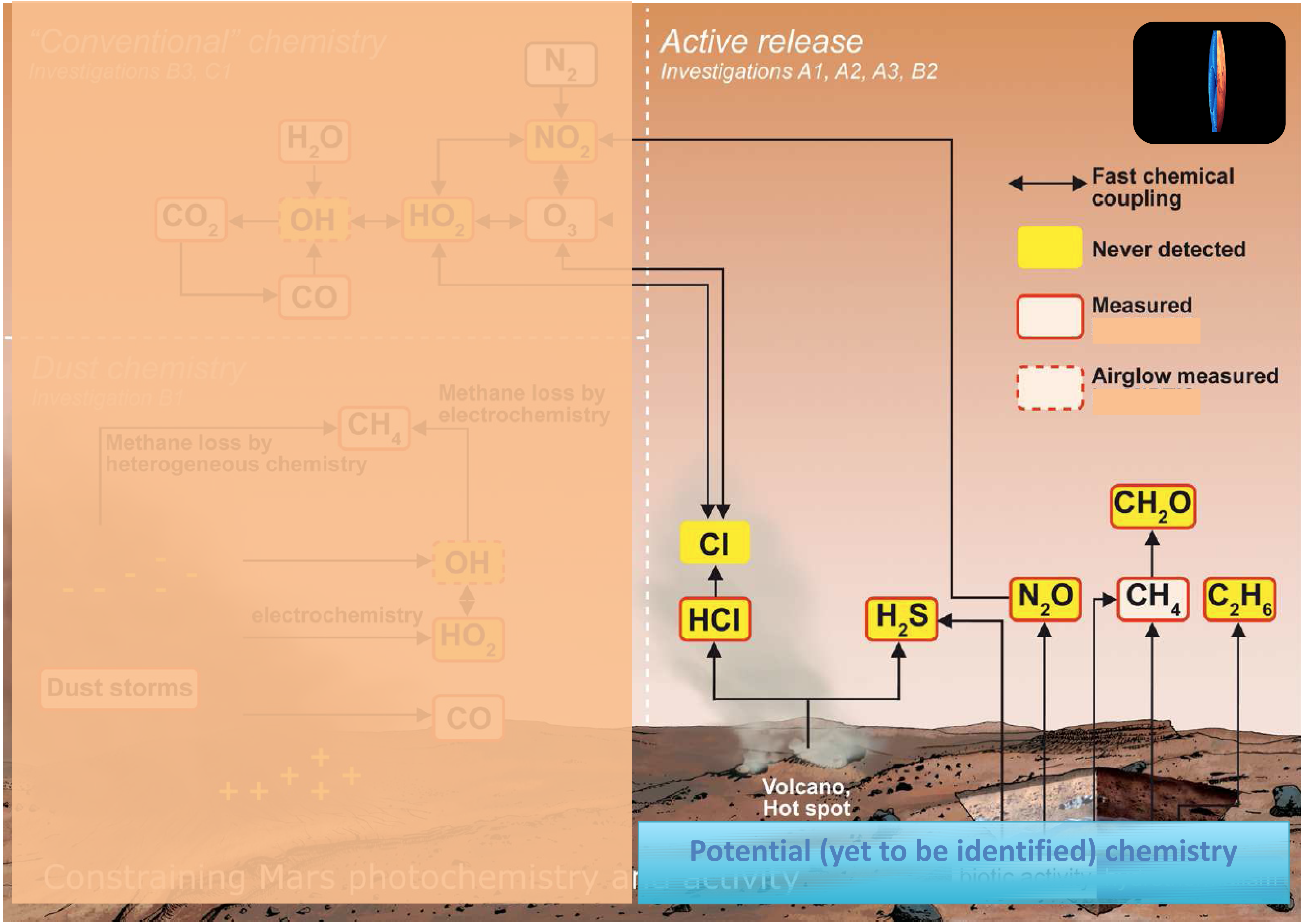

Constraining Mars photochemistry and activity

Potential (yet to be identified) chemistry

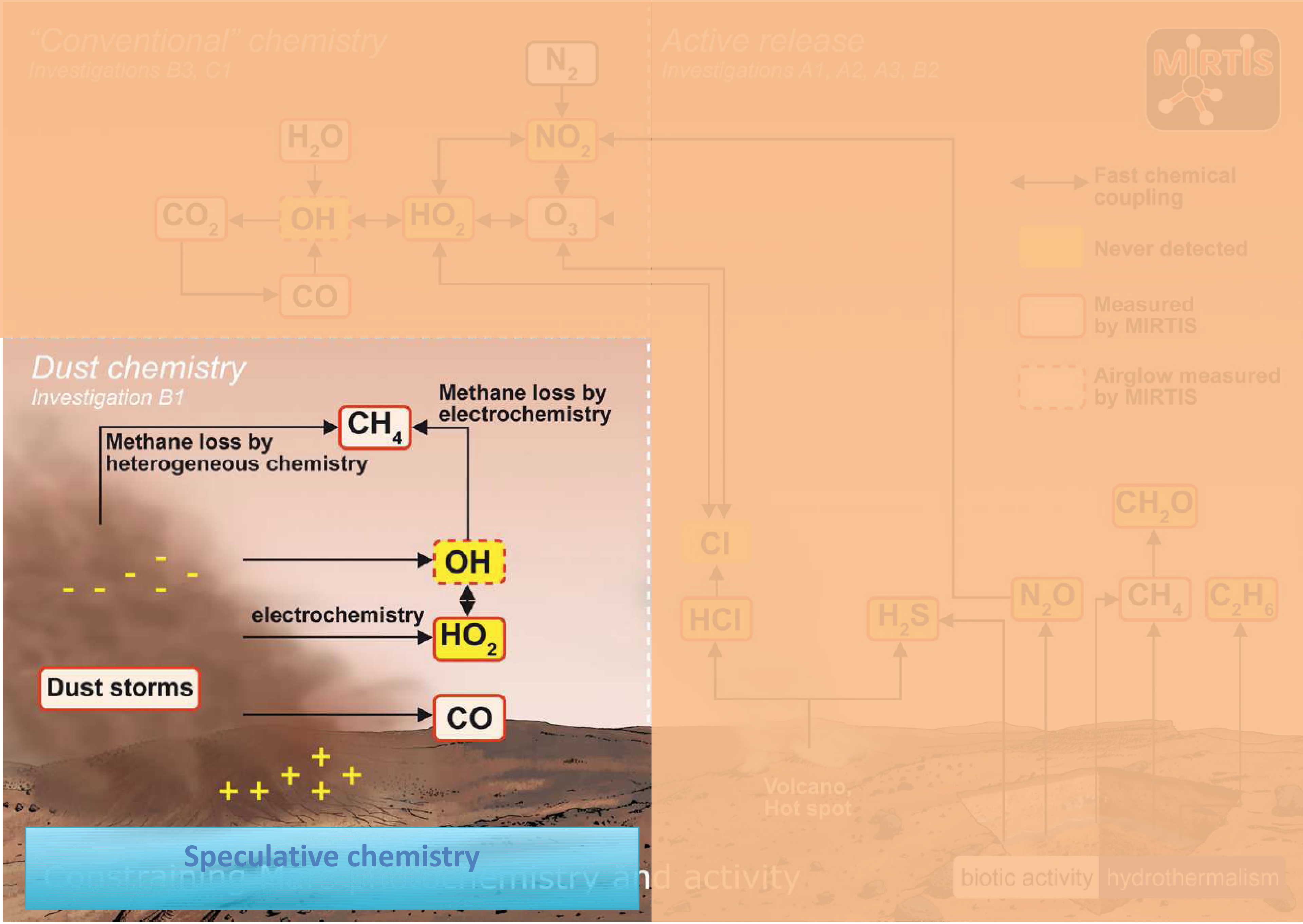

"Conventional" chemistry

Investigations B3, C1

N_2

NO_2

H_2O

CO_2

OH

HO_2

O_3

CO

Active release

Investigations A1, A2, A3, B2

Fast chemical coupling

Never detected

Measured by MIRTIS

Airglow measured by MIRTIS

Cl

HCl

H_2S

N_2O

CH_4

C_2H_6

CH_2O

Volcano, Hot spot

biotic activity

hydrothermalism

Dust chemistry

Investigation B1

Methane loss by electrochemistry

Methane loss by heterogeneous chemistry

CH_4

OH

electrochemistry

HO_2

Dust storms

CO

Speculative chemistry

Constraining Mars photochemistry and activity

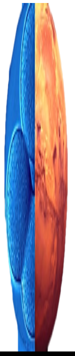

The case of Halogen species

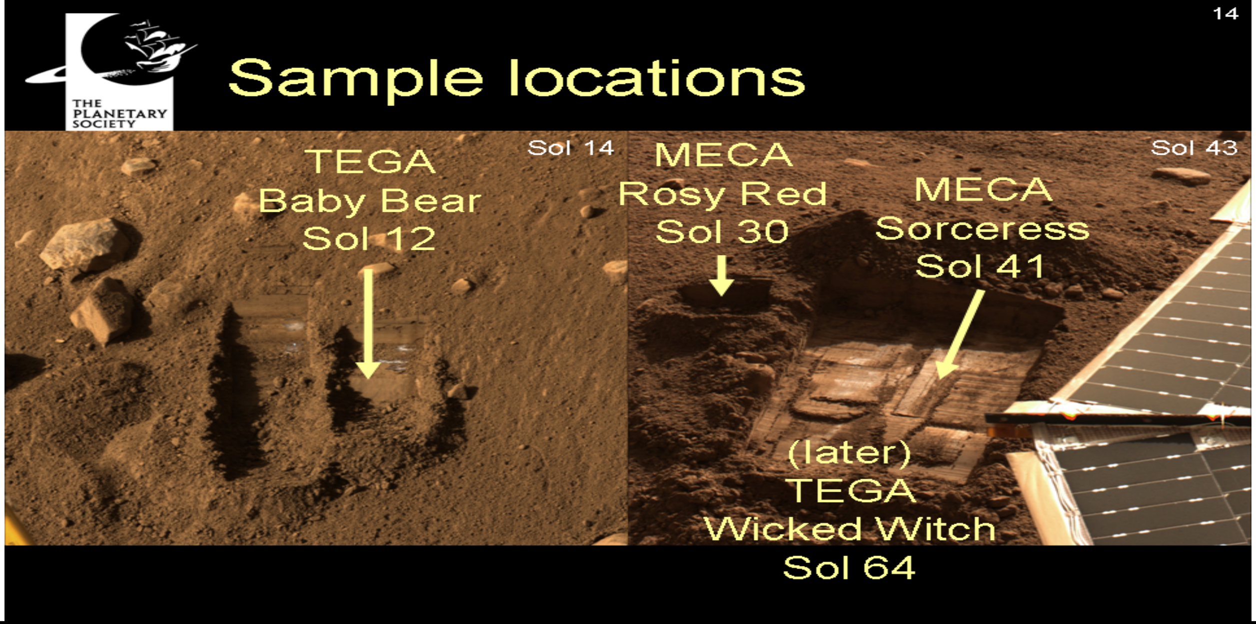

Sample locations

Detection of perchlorate (ClO4-) by Phoenix MECA experiment is indicative of Cl species once outgassed into the atmosphere

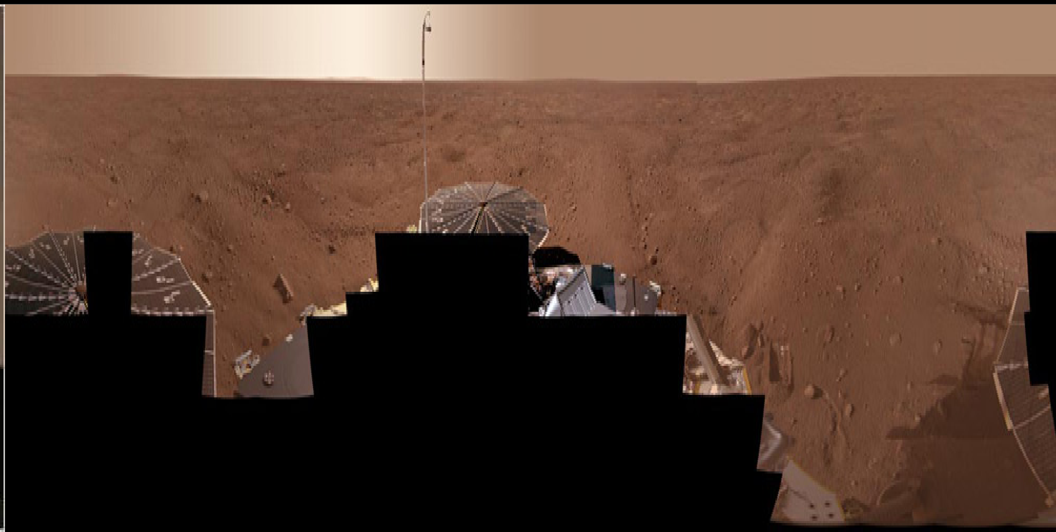

HCl, HF, HBr, etc….

None of these species have been detected to date.

Upper limits on HCl and H_2O_2

Herschel latest results give an upper limit of ~200 ppt for HCl

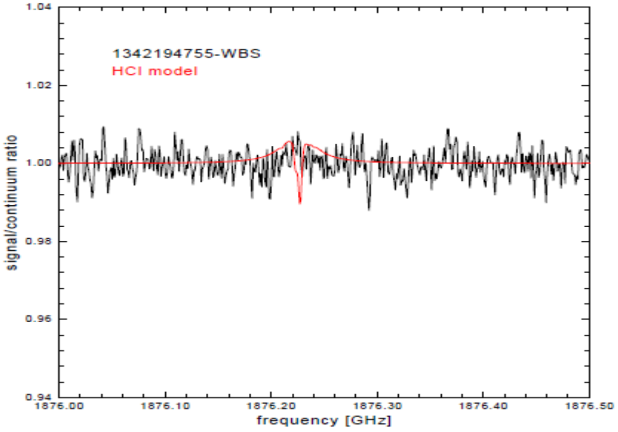

< 200 ppt

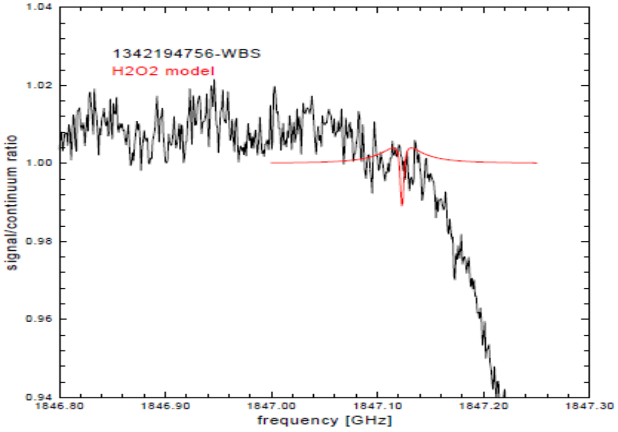

< 2 ppb

Hartogh et al. 2010, A&A

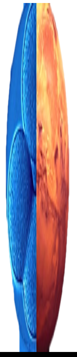

The case of Sulfur species

Cliquez pour modifier le style des sous-titres du masque

Sulfur species on Mars

- Sulfur species found at the surface
  - Viking: sulfates in the soil (5-10%, Toulmin et al. 1977)
  - Spirit & Opportunity: sulfates minerals (>10%, Squyres et al. 2004)
  - OMEGA/MEx: Calcium sulfate (gypsum) identified at high N-latitudes (Langevin et al. 2005)
- However, no sulfur-bearing molecule has been found in the atmosphere
  - OCS < 70 ppb
  - H2S < 20 ppb
  - SO2 < 1 ppb thermal IR (Krasnopolsky 2005)
  - SO2 < 2 ppb submm (Nakagawa et al. 2009)

Encrenaz et al., 2011

Sulfur species on Mars

- Sulfur species found at the surface
  - Viking: sulfates in the soil (5-10%, Toulmin et al. 1977)
  - Spirit & Opportunity: sulfates minerals (>10%, Squyres et al. 2004)
  - OMEGA/MEx: Calcium sulfate (gypsum) identified at high N-latitudes (Langevin et al. 2005)
- However, no sulfur-bearing molecule has been found in the atmosphere
  - **OCS < 70 ppb**
  - **H2S < 20 ppb**
  - **SO2 < 1 ppb** **thermal IR (Krasnopolsky 2005)**
  - **SO2 < 2 ppb** **submm (Nakagawa et al. 2009)**

Encrenaz et al., 2011

SO2 upper limit – Krasnopolsky, Icarus 178, 48, 2005

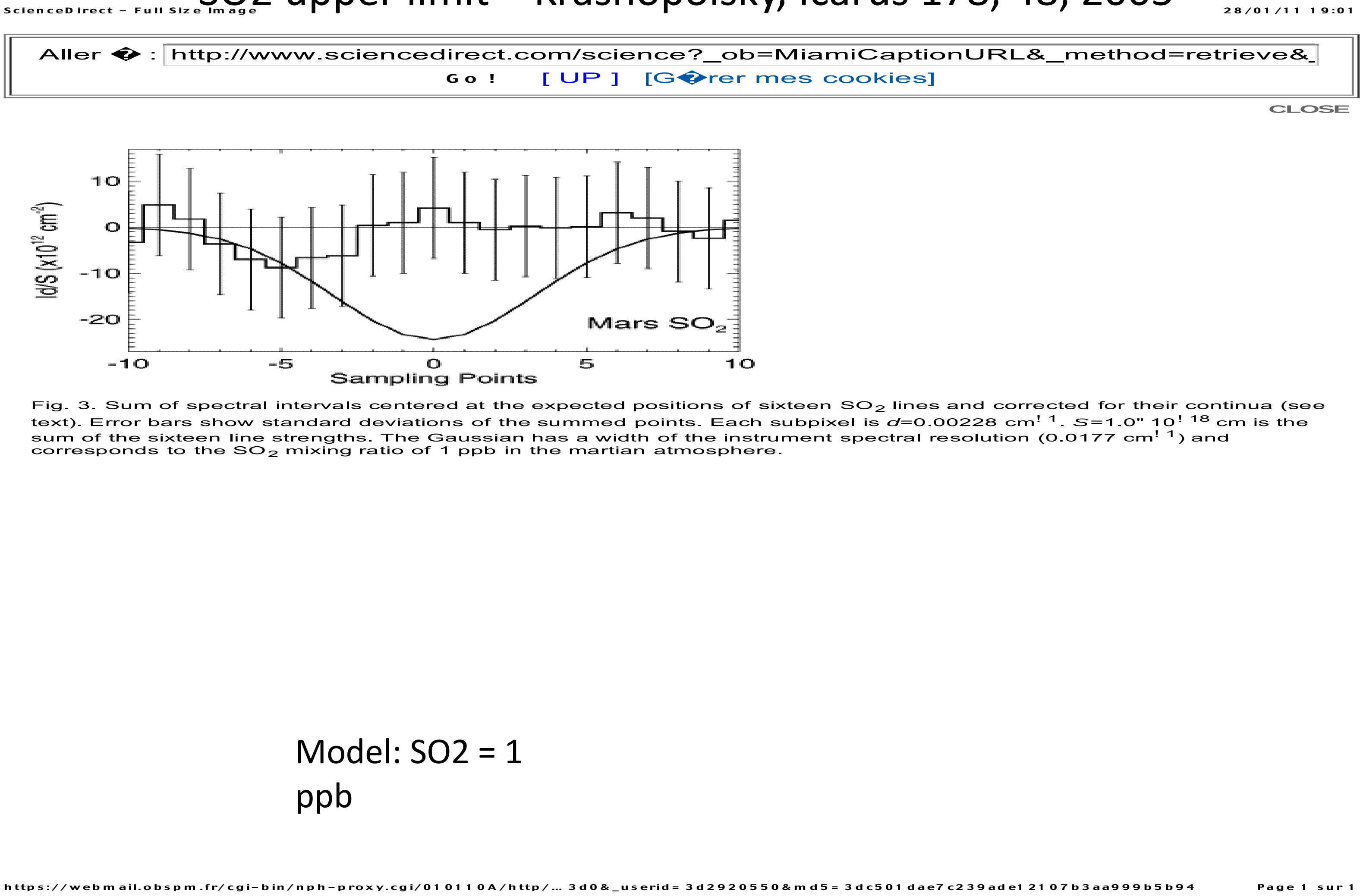

http://www.sciencedirect.com/science?_ob=MiamiCaptionURL&_method=retrieve&_

Fig. 3. Sum of spectral intervals centered at the expected positions of sixteen SO_2 lines and corrected for their continua (see text). Error bars show standard deviations of the summed points. Each subpixel is $d=0.00228\ \mathrm{cm}^{-1}$. $S=1.0\times10^{-18}$ cm is the sum of the sixteen line strengths. The Gaussian has a width of the instrument spectral resolution ($0.0177\ \mathrm{cm}^{-1}$) and corresponds to the SO_2 mixing ratio of 1 ppb in the martian atmosphere.

https://webmail.obspm.fr/cgi-bin/nph-proxy.cgi/010110A/http/... 3d0&_userid=3d2920550&md5=3dc501dae7c239ade12107b3aa999b5b94

Model: SO2 = 1
ppb

SO2 < 1 ppb (2s) – Integration over Tharsis region
Ls = 205° (June 2003)

Encrenaz et al., 2011

Search for SO2 using high-resolution imaging spectroscopy in the thermal infrared

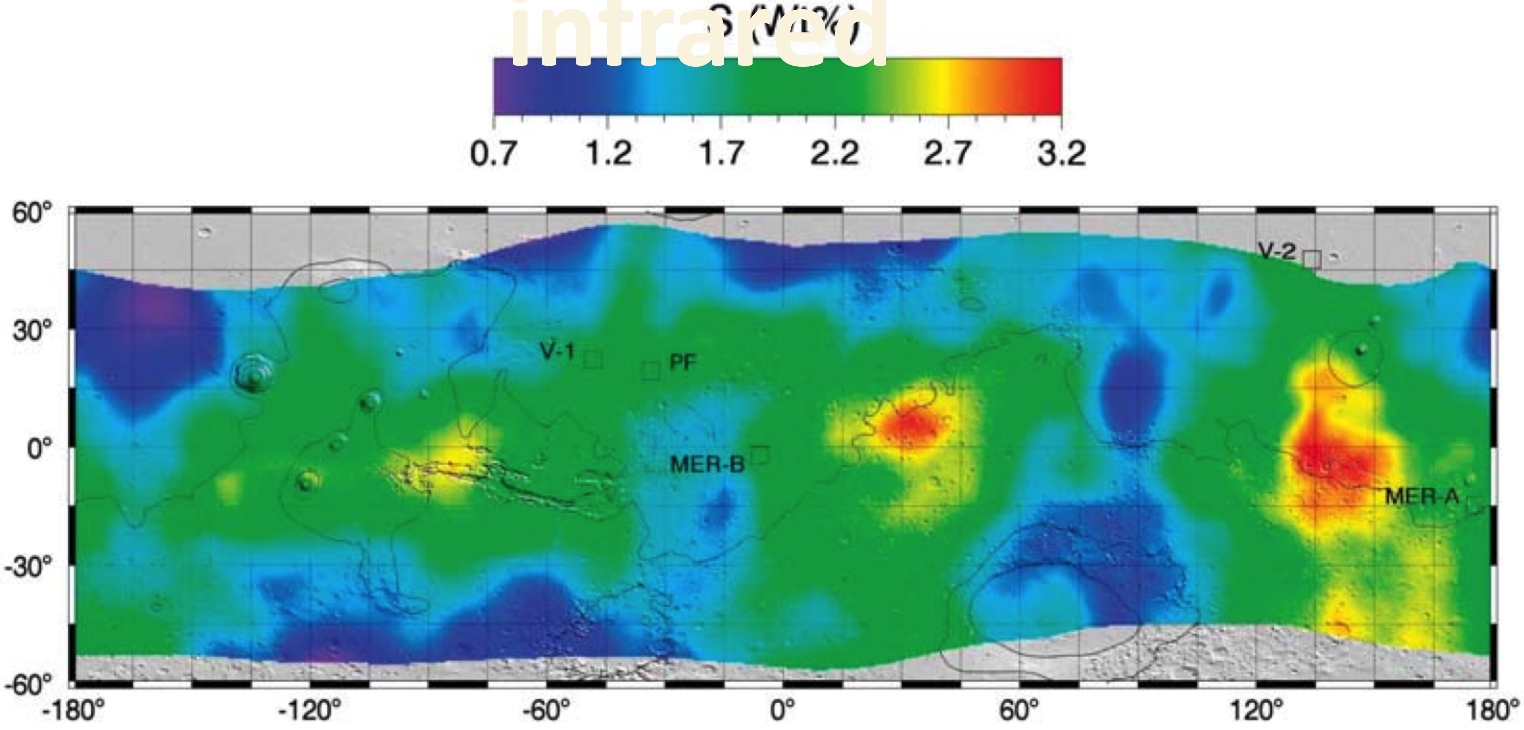

Instrumen

Spectral range:	7.35 - 7.40 µm
Spectral resolving power:	84000
Spatial resolution:	1 arcsec
Date:	12 october 2009
Ls:	352° (equinox)
Mars diameter:	6 arcsec

Encrenaz et al., 2011

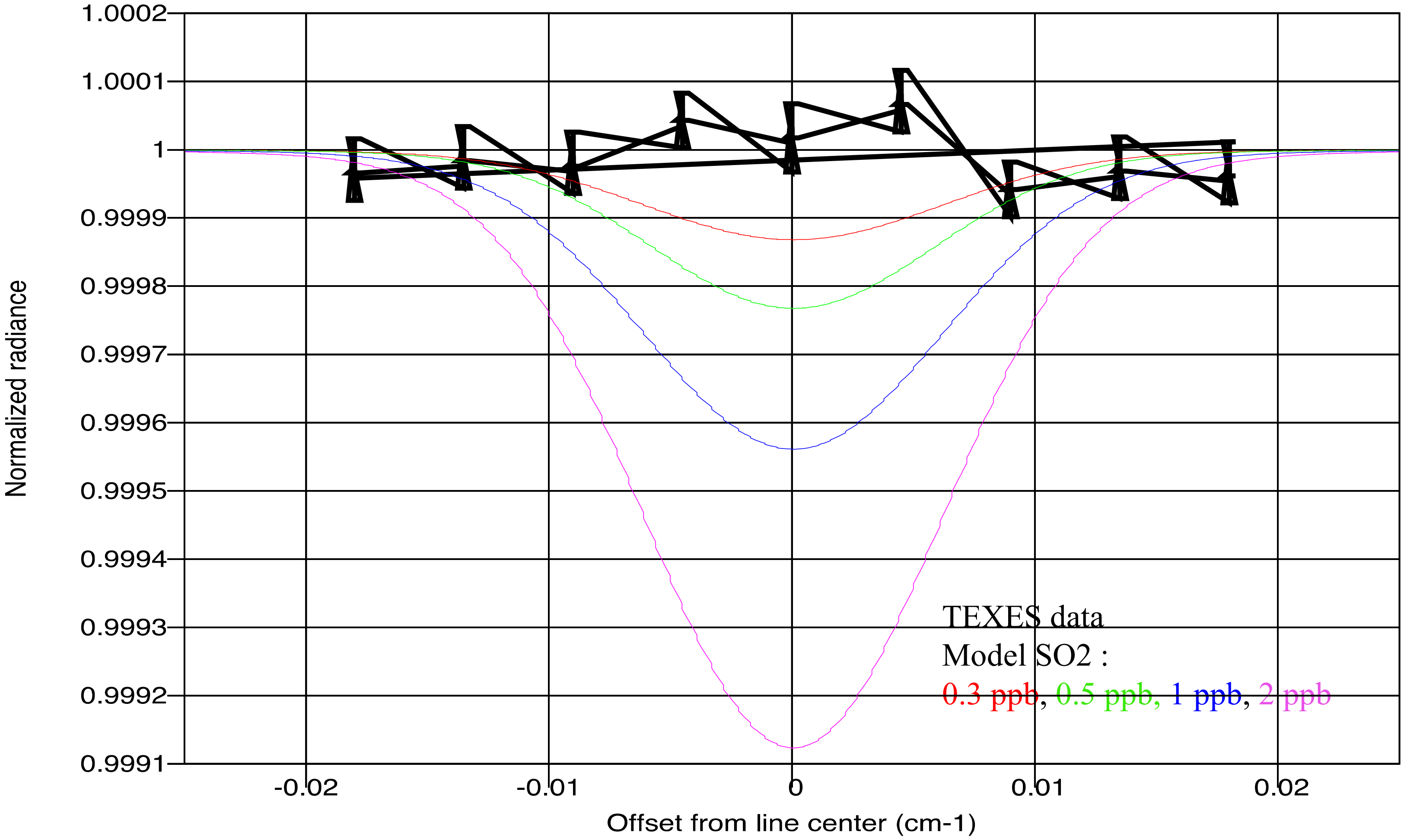

2σ upper limit : SO2 < 0.3 ppb

Encrenaz et al., 2011

SO2 upper limit over the Martian disk

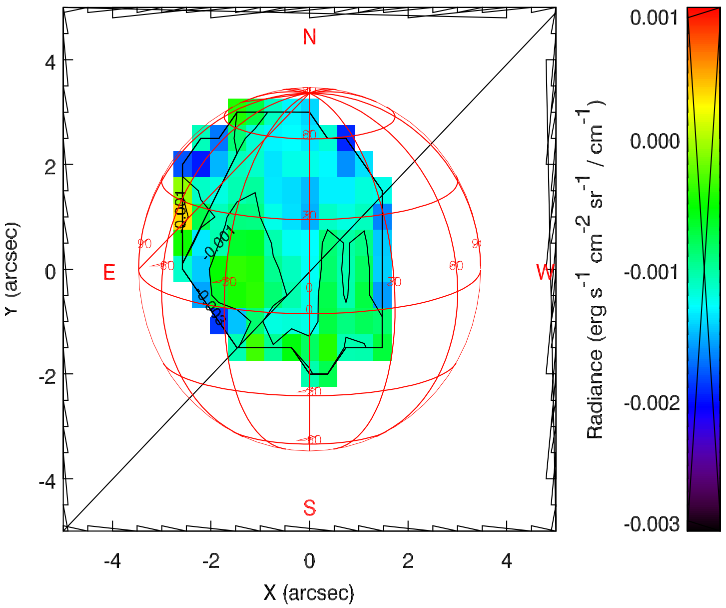

Long(Central Meridian)= 140 E

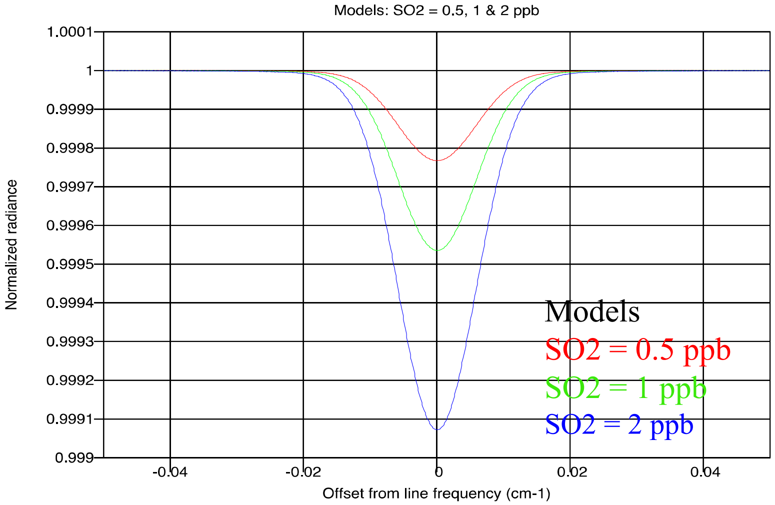

Line depth = 0.001 -> SO2 = 2 ppb

SO2 < 2 ppb everywhere on the disk
in particular at high N-latitudes

Region observed:

Long: 50-170 E, lat > 30N
Long: 100-170 E, 0 < lat <30N
Long: 110-170 E, 15S < lat < 0

Conclusions for sulfur species

- SO2 upper limit (2σ): 0.3 ppb at mid-northern latitudes,
  2 ppb at all northern latitudes
- SO2 is a non-condensible species with lifetime (2 yr) longer than global mixing (0.5 y)
  - homogeneous distribution is expected
- **No evidence for localized sources**
  - even around gypsum region
  - consistent with above statement (S-rich areas are not tracers of gaseous SO2)
- No evidence for seepage at the Martian surface
  - SO2/CH4 typically 10-4 – 10-3 in Earth volcanoes
  - If CH4 is present on Mars, seepage origin seems unlikely (cf. Krasnopolsky 2005)

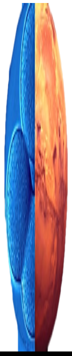

The case of Methane

Cliquez pour modifier le style des sous-titres du masque

Detection of Methane in the Atmosphere of Mars

Vittorio Formisano,[1]* Sushil Atreya,[2] Thérèse Encrenaz,[3]
Nikolai Ignatiev,[4,1] Marco Giuranna[1]

We report a detection of methane in the martian atmosphere by the Planetary Fourier Spectrometer onboard the Mars Express spacecraft. The global average methane mixing ratio is found to be 10 ± 5 parts per billion by volume (ppbv). However, the mixing ratio varies between 0 and 30 ppbv over the planet. The source of methane could be either biogenic or nonbiogenic, including past or present subsurface microorganisms, hydrothermal activity, or cometary impacts.

Methane (CH_4) is an important tracer of possible biological, internal, or atmospheric processes on Mars. The possibility of methane-producing bacteria or microorganisms on Mars has been suggested in the past (*1*, *2*). The source of methane could also be in water/rock reactions in the martian interior (*3*, *4*) or volcanic hot spots (*5*). Another possibility is external sources such as cometary impacts (*6*).

The Planetary Fourier Spectrometer (PFS) (*7*) operates in the infrared, covering a wavelength range of 1.2 to 45 μm (220 to 8190 cm^{-1}) in two spectral channels: the short wavelength (SW), from 1.2 to 5.5 μm, and the long wavelength (LW), from 5.5 to 45 μm (*8*, *9*). The spectral resolution is 1.3 cm^{-1} and the spatial resolution is ~10 km near the pericenter. Sampling is done every 1.02 cm^{-1}. Four bands of methane lie within the spectral range of the PFS, at 1300, 3000, 4400, and 6000 cm^{-1}. The 6000 cm^{-1} band is not suitable for detecting weak CH_4 signatures by the PFS because of the presence of many strong solar Fraunhofer lines and the lack of a reference solar spectrum in this region to subtract these lines. In the 4400 and 1300 cm^{-1} regions, there is some evidence of spectral signatures of minor species. However, the signal-to-noise ratio (SNR) (*10*) of the PFS is much greater in the 3000 cm^{-1} region. Therefore, we have searched for methane in this band (ν_3), centered at 3018 cm^{-1}, which is also the strongest fundamental band of methane. To increase the SNR, we first averaged data from 16 orbits obtained in January-February 2004 (*11*), covering the entire longitude range. For 16 orbits, about 100 spectra were selected in the equatorial region where a high radiance level is expected, and a total of 1680 spectra were averaged together to obtain a global spectrum (Fig. 1A). An average of 2931 spectra taken in 24 orbits during a following period in May 2004 is shown in Fig. 1B.

The electronic noise of the instrument providing a 1σ (67%) confidence level in the measurements was computed from measurements of deep space. For the SW channel of the PFS, deep space corresponds to a source of radiance intensity zero; hence it provides a measure of the instrumental noise (*10*). The noise equivalent radiance (NER) of a single spectrum at 3000 cm^{-1} is 0.01 erg/(s sr cm^2 cm^{-1}). Accordingly, the S/N ratios for our two data sets are about 1300 (Fig. 1A) and 1500 (Fig. 1B), respectively. A number of solar and water vapor lines can be identified in the spectrum. However, certain features, particularly the ones at 3006.5, 3009, and 3018 cm^{-1}, are not associated with any presently known molecules of the martian atmosphere. Figure 2, A and B, shows a comparison of the averaged data, with synthetic spectra calculated with a mean H_2O mixing ratio of 350 parts per million (ppm). With a depth of about 1% (that is, more than 10 times above the noise level), the line at 3018 cm^{-1} is significant, because it corresponds to the line position of maximum methane absorption in this wavenumber region (ν_3-Q branch). We identified this feature with methane by comparing it to a synthetic spectrum (*12*, *13*) (red curve in Fig. 2), and determined the abundance of methane in the atmosphere from the line depth. Other methane lines present in this region have been checked but are found to be less intense than the one presented here by at least a factor of 3 to 4. Many are hidden in water or solar lines. One of them, at 3028 cm^{-1}, is shown in the figures. Its behavior is similar to that of the main line at 3018 cm^{-1}; however, it is too weak for evaluating the mixing ratio, and it is also partially contaminated by water vapor lines.

At 3011 cm^{-1}, on the left side of a strong solar line, the discrepancy between the observed and synthetic spectra reflects an instrumental ("overshooting") effect that is frequently present in the PFS spectra in the red wing of single strong lines. Apart from this departure, a possible explanation for the discrepancies observed at other frequencies (3002, 3007, and 3009 cm^{-1}) is that they are due to unidentified minor molecular species. Further discrepancies can be due to (i) H_2O spectroscopic parameters or insufficient mixing ratio or (ii) surface albedo (which, in the 3000 cm^{-1} range, can be affected by mineralogic signatures of hydrated minerals). However, we believe that the identification of methane at 3018 cm^{-1} is definite, in view of the good fit of its wavenumber position.

The slope of the synthetic spectrum of the martian atmosphere (Fig. 2, A and B) indicates the presence of water ice clouds in the equatorial region of Mars. Indeed, the quality of the fits improves when such clouds are included in the synthetic spectra. In the synthetic spectra, the water ice cloud particles have an effective dimension of 1.25 μm (*14*), and optical constants from (*15*) have been used. From the direct comparison between the PFS spectra and the synthetic spectra (Fig. 2, A and B), we find that the observed line depth corresponds to a methane mixing ratio of approximately 10 parts per billion by volume (ppbv) or somewhat greater. Considering the uncertainty of the fitting with the synthetic spectrum (*10*), we derive a conservative CH_4 mixing ratio of 10 ± 5 ppbv (*16*). The synthetic calculations also show that because the individual lines are not saturated, the depth of the ν_3-Q branch should increase almost linearly with increasing mixing ratio, and this fact can be used to identify and study variations of the methane mixing ratio.

An examination of orbits with a higher air-mass factor can provide greater confidence in our analysis, because the methane line depth should increase with increasing amounts of CH_4 along the line of sight. This is possible to do because occasionally Mars Express does not point to the nadir, its normal operation mode, but at a slant angle due to its inertial attitude. This results in an increased air mass in the line of sight, which implies that the line of sight abundance of methane should also increase, whereas its mixing ratio is expected to remain unchanged. The average spectrum over 121 measurements taken during the

---

[1]Istituto di Fisica dello Spazio Interplanetario INAF-IFSI, Via del Fosso del Cavaliere 100, 00133 Rome, Italy. [2]Department of Atmospheric, Oceanic, and Space Sciences, University of Michigan, Ann Arbor, MI 48109–2143, USA. [3]Laboratoire d'Etudes Spatiales et d'Instrumentation en Astrophysique (LESIA), Observatoire de Paris, 5 Place Janssen, 92195 Meudon, France. [4]Space Research Institute of Russian Academy of Sciences (IKI) Profsojuznaja 84/32, 117810 Moscow, Russia.

*To whom correspondence should be addressed. E-mail: formisan@nike.ifsi.rm.cnr.it

---

pericenter pass of orbit 145, with an air-mass factor of 1.12, is shown in Fig. 3. Upon taking into account the air-mass factor, we obtain a methane mixing ratio of 30 ± 5 ppbv. This value is higher than the global average ratio of 10 ± 5 ppbv and indicates that the methane mixing ratio may be variable. Motivated by this possibility, we have examined several other orbits, including orbit 68, 202, and 72, for which the air-mass factors are, respectively, 1.03, 1.33, and 2.1. We discovered that orbit 72, for which the air-mass factor (2.1) was even greater than in orbit 145 (1.12), gives another extreme in CH_4. Because the number of measurements for this case (120) is close to those in orbit 145, a similar sigma value is obtained. Figure 4 gives the average PFS spectrum for orbit 72. However, there is no indication of the methane line, and the synthetic spectrum with no methane fits the data nicely. Because the synthetic spectrum fitting orbit 72 data has been computed using the same solar spectrum as we used for other fits, this indicates that the 3018 cm^{-1} line was not due to the Sun. From the four orbits 68, 145, 202, and 72, with respective air-mass factors of 1.03, 1.12, 1.33, and 2.1, methane mixing ratios of 9, 30, 30, and 0 ppbv are derived by comparing the observed methane line depth to synthetic spectra, after taking into account the air-mass factors. In the case of orbit 72, we conclude that the methane abundance is below our detectability limit: lower than 5 ppbv.

The above variation in CH_4 could represent either spatial or temporal changes or both. Because the time span of our observations (January through May 2004) is short compared to the martian year (almost 2 Earth years) and seasons (about 6 months each), the CH_4 variation mentioned above can be studied versus spatial changes. Space variations could be present because of localized sources and/or localized surface sinks. We can attempt to determine whether the spatial variations occur over a large range of longitude by dividing our original 16 orbits (or 24 orbits) into three longitudinal ranges: longitudes −55° to −170° (orbits 10, 30, 32, 41, *44*, and *202*); longitudes +52° to −55° (orbits 20, 61, 100, 103, *145*, and 148); and longitudes +52° to +190° (orbits 24, 71, *72*, and 97) (the numbers in italics represent inertial orbits) (Fig. 5). The three sets of orbits for the second group are as follows: longitudes −55° to −170° (orbits *390*, 386, 394, 397, *400*, and 401); longitudes +52° to −55° (orbits *404*, 405, *408*, *410*, 411, 426, 427, *428*, *429*, 430, and *431*); longitudes +52° to +19° (orbits *414*, *417*, 418, 420, 421, 424, and 425) (the numbers in italics represent inertial orbits). The three sets of longitudes are presented in different colors in Fig. 5.

The methane mixing ratio decreases from group 1 to group 3 (Fig. 6). The best fit is obtained for the methane mixing ratios of 25 ± 5, 15 ± 5, and 10 ± 5 ppbv, respectively, for the three longitude ranges, going from eastern longitudes to western longitudes. However, orbit 145 in group 2 has the highest mixing ratio of any individual orbit, implying that methane concentrations can be high in smaller regions within these longitudinal ranges.

Previously, an upper limit of 20 ppbv of methane was obtained by Mariner 9 (*17*), and another one of 70 ± 50 ppbv was inferred from ground-based observations (*18*). However, recently two ground-based detections of methane were reported (*19*, *20*) with a mixing ratio of 11 ± 4 ppbv (*20*), in agreement with the Mars Express PFS result for the global methane mixing ratio.

CH4 band

On Earth, the dominant source of methane is biogenic sources such as termites and cattle (*21*). Other sources of terrestrial methane include marshes, rice paddles, natural gas, lakes, and oceans. On Mars, methane could be derived from biogenic sources such as subsurface microorganisms (*1*) or nonbiogenic sources such as the slow release of methane stored in subsurface reservoirs, outgassing from volcanic/hydrothermal reservoirs, or the destruction of meteoritic or cometary material during infall. We estimated the global methane mixing ratio produced by each of these sources. The observed global average mixing ratio of 10 ppbv amounts to a column abundance of 2.2 × 10^{15} cm^{-2} CH_4 molecules at the surface of Mars. Assuming a CH_4 photochemical lifetime of ~2 × 10^{10} s near the surface (*5*, *23*) we estimate that a flux of ~1 × 10^5 molecules cm^{-2} s^{-1} would be required to explain a CH_4 mixing ratio of 10 ppb on Mars (*16*). Integrated over the planet, this would amount to a methane source strength of ~4 g s^{-1}; that is, ~1.26 × 10^5 kg year^{-1} or ~126 tons year^{-1}.

The flux of micrometeoritic dust at Mars is estimated to be ~300 g s^{-1} or ~9000 tons year^{-1} (*24*). Most of it would burn up in the atmosphere, but allowing for a generous 25% surviving to the surface (*24*), nearly 2300 tons year^{-1} could reach the surface of Mars. If all of the micrometeoritic dust is assumed to be from carbonaceous chondrites, then organic materials would comprise about 3% of the flux (*25*): ~70 tons year^{-1}. If all of the organic materials could be converted to methane, then micrometeoritic sources of methane would be roughly comparable to that needed to explain

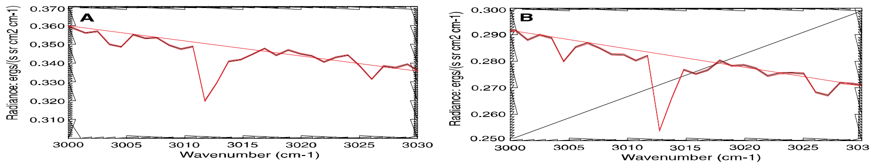

Fig. 1. **(A)** A portion of the first averaged PFS spectrum (January-February 2004, black curve), with ±1σ confidence (red lines). The SNR is about 1300. Methane is identified at 3018 cm^{-1}. There are three water lines (at 3003.5, 3022, and 3026 cm^{-1}) and two solar lines (at 3012 and 3014 cm^{-1}). The continuum slope is due to water ice clouds in the atmosphere. The small peak at the left of the main solar line is due to instrumental response function. **(B)** The second averaged PFS spectrum (May 2004) in the same frequency interval. The caption is the same as for (A). The SNR is about 1500.

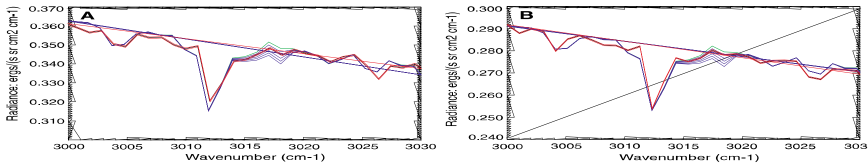

Fig. 2. **(A)** Synthetic spectra computed for 0 ppbv (green curve) and 10, 20, 30, 40, and 50 ppbv (violet curves) of methane, compared with the PFS average spectrum (black curve). The synthetic spectra have been computed for 6.7 millibars of CO_2, including 350 ppm of H_2O, along with dust and water ice clouds. The temperature profile obtained from simultaneous measurements in the thermal radiation was used. **(B)** Same as (A), with the PFS mean spectrum shown in Fig. 1B.

janvier-février 2004

Ls = 330-350°

mai 2004

Ls = 30°

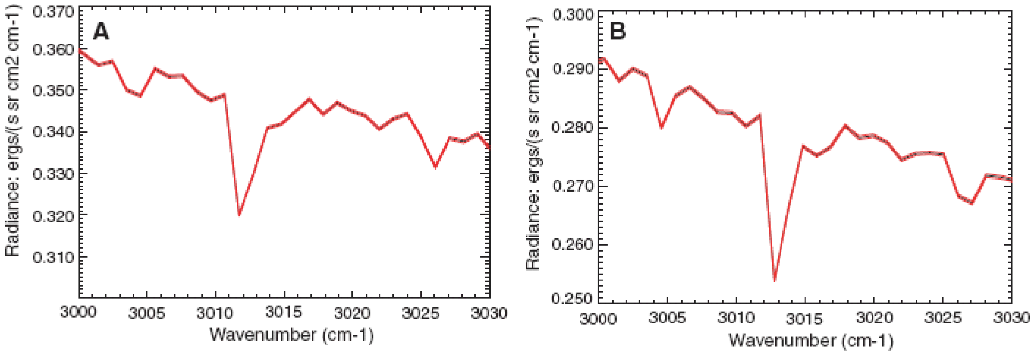

Fig. 1. (**A**) A portion of the first averaged PFS spectrum (January-February 2004, black curve), with $\pm 1\sigma$ confidence (red lines). The SNR is about 1300. Methane is identified at 3018 cm^{-1}. There are three water lines (at 3003.5, 3022, and 3026 cm^{-1}) and two solar lines (at 3012 and 3014 cm^{-1}). The continuum slope is due to water ice clouds in the atmosphere. The small peak at the left of the main solar line is due to instrumental response function. (**B**) The second averaged PFS spectrum (May 2004) in the same frequency interval. The caption is the same as for (A). The SNR is about 1500.

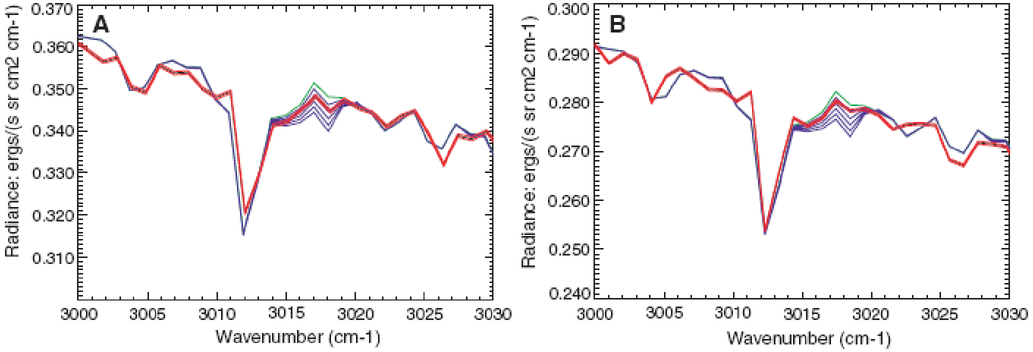

Fig. 2. (**A**) Synthetic spectra computed for 0 ppbv (green curve) and 10, 20, 30, 40, and 50 ppbv (violet curves) of methane, compared with the PFS average spectrum (black curve). The synthetic spectra have been computed for 6.7 millibars of CO_2, including 350 ppm of H_2O, along with dust and water ice clouds. The temperature profile obtained from simultaneous measurements in the thermal radiation was used. (**B**) Same as (A), with the PFS mean spectrum shown in Fig. 1B.

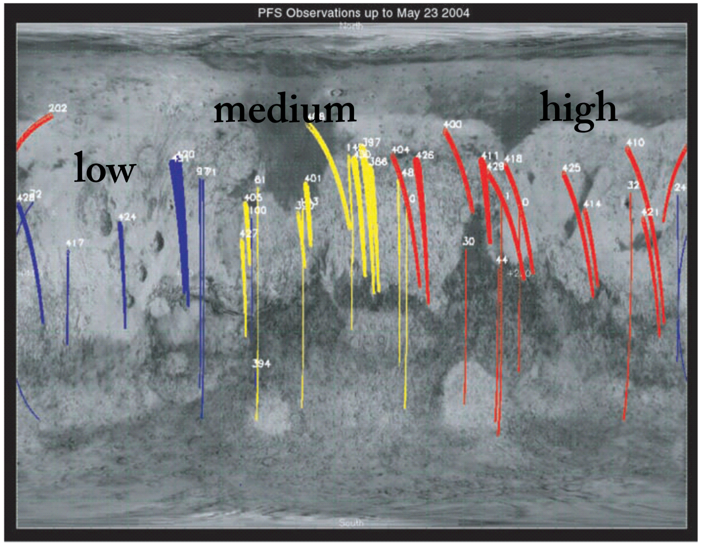

Fig. 5. Geographical distribution of the orbits considered: red (high methane mixing ratio), yellow (medium methane mixing ratio), and blue (low methane mixing ratio). Strong fluctuations occur in each of the three categories, indicating the possible presence of localized sources.

Global Average: 10 ± 5 ppbv

2009: Groundbased Observations

(MUMMA et al., 2009)

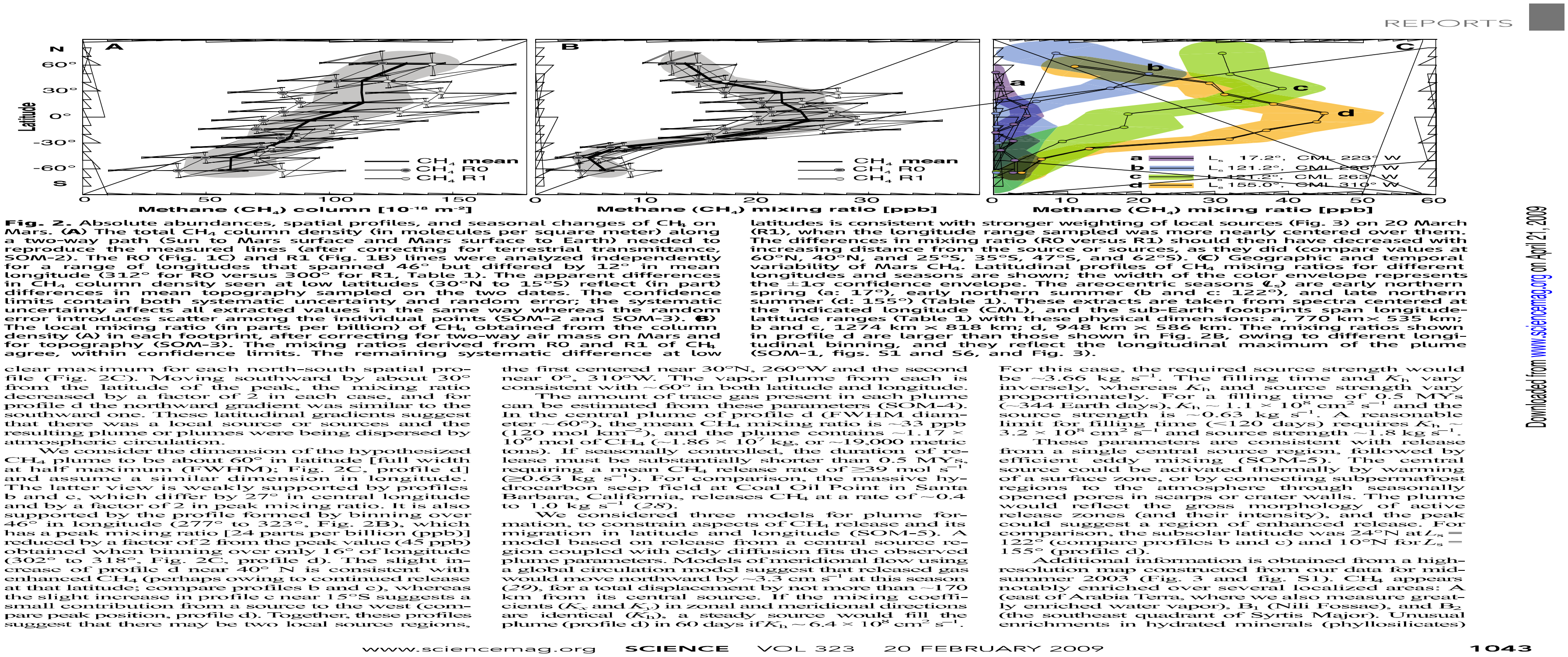

Fig. 2. Absolute abundances, spatial profiles, and seasonal changes of CH$_4$ on Mars. **(A)** The total CH$_4$ column density (in molecules per square meter) along a two-way path (Sun to Mars surface and Mars surface to Earth) needed to reproduce the measured lines (after correcting for terrestrial transmittance, SOM-2). The R0 (Fig. 1C) and R1 (Fig. 1B) lines were analyzed independently for a range of longitudes that spanned 46° but differed by 12° in mean longitude (312° for R0 versus 300° for R1, Table 1). The apparent differences in CH$_4$ column density seen at low latitudes (30°N to 15°S) reflect (in part) differences in mean topography sampled on the two dates. The confidence limits contain both systematic uncertainty and random error; the systematic uncertainty affects all extracted values in the same way whereas the random error introduces scatter among the individual points (SOM-2 and SOM-3). **(B)** The local mixing ratio (in parts per billion) of CH$_4$ obtained from the column density (A) in each footprint, after correcting for two-way air mass on Mars and for topography (SOM-3). The mixing ratios derived from R0 and R1 of CH$_4$ agree, within confidence limits. The remaining systematic difference at low latitudes is consistent with stronger weighting of local sources (Fig. 3) on 20 March (R1), when the longitude range sampled was more nearly centered over them. The differences in mixing ratio (R0 versus R1) should then have decreased with increasing distance from the source or sources, as they did (compare values at 60°N, 40°N, and 25°S, 35°S, 47°S, and 62°S). **(C)** Geographic and temporal variability of Mars CH$_4$. Latitudinal profiles of CH$_4$ mixing ratios for different longitudes and seasons are shown; the width of the color envelope represents the ±1σ confidence envelope. The areocentric seasons (L_s) are early northern spring (a: 17°), early northern summer (b and c: 122°), and late northern summer (d: 155°) (Table 1). These extracts are taken from spectra centered at the indicated longitude (CML), and the sub-Earth footprints span longitude-latitude ranges (Table 1) with these physical dimensions: a, 770 km × 535 km; b and c, 1274 km × 818 km; d, 948 km × 586 km. The mixing ratios shown in profile d are larger than those shown in Fig. 2B, owing to different longitudinal binning, and they reflect the longitudinal maximum of the plume (SOM-1, figs. S1 and S6, and Fig. 3).

clear maximum for each north-south spatial profile (Fig. 2C). Moving southward by about 30° from the latitude of the peak, the mixing ratio decreased by a factor of 2 in each case, and for profile d the northward gradient was similar to the southward one. These latitudinal gradients suggest that there was a local source or sources and the resulting plume or plumes were being dispersed by atmospheric circulation.

We consider the dimension of the hypothesized CH$_4$ plume to be about 60° in latitude [full width at half maximum (FWHM); Fig. 2C, profile d] and assume a similar dimension in longitude. The latter view is weakly supported by profiles b and c, which differ by 27° in central longitude and by a factor of 2 in peak mixing ratio. It is also supported by the profile formed by binning over 46° in longitude (277° to 323°, Fig. 2B), which has a peak mixing ratio [24 parts per billion (ppb)] reduced by a factor of 2 from the peak value (45 ppb) obtained when binning over only 16° of longitude (302° to 318°, Fig. 2C, profile d). The slight increase of profile d near 40° N is consistent with enhanced CH$_4$ (perhaps owing to continued release at that latitude; compare profiles b and c), whereas the slight increase in profile c near 15°S suggests a small contribution from a source to the west (compare peak position, profile d). Together, these profiles suggest that there may be two local source regions, the first centered near 30°N, 260°W and the second near 0°, 310°W. The vapor plume from each is consistent with ~60° in both latitude and longitude.

The amount of trace gas present in each plume can be estimated from these parameters (SOM-4). In the central plume of profile d (FWHM diameter ~60°), the mean CH$_4$ mixing ratio is ~33 ppb (120 mol km^{-2}), and the plume contains ~1.17×10^9 mol of CH$_4$ (~1.86×10^7 kg, or ~19,000 metric tons). If seasonally controlled, the duration of release must be substantially shorter than 0.5 MYs, requiring a mean CH$_4$ release rate of ≥39 mol s^{-1} (≥0.63 kg s^{-1}). For comparison, the massive hydrocarbon seep field at Coal Oil Point in Santa Barbara, California, releases CH$_4$ at a rate of ~0.4 to 1.0 kg s^{-1} (*28*).

We considered three models for plume formation, to constrain aspects of CH$_4$ release and its migration in latitude and longitude (SOM-5). A model based on release from a central source region coupled with eddy diffusion fits the observed plume parameters. Models of meridional flow using a global circulation model suggest that released gas would move northward by ~3.3 cm s^{-1} at this season (*29*), for a total displacement by not more than ~170 km from its central source. If the mixing coefficients (K_x and K_y) in zonal and meridional directions are identical (K_h), a steady source would fill the plume (profile d) in 60 days if $K_h \sim 6.4 \times 10^8$ cm^2 s^{-1}. For this case, the required source strength would be ~3.66 kg s^{-1}. The filling time and K_h vary inversely, whereas K_h and source strength vary proportionately. For a filling time of 0.5 MYs (~344 Earth days), $K_h \sim 1.1 \times 10^8$ cm^2 s^{-1} and the source strength is ~0.63 kg s^{-1}. A reasonable limit for filling time (<120 days) requires $K_h \sim 3.2 \times 10^8$ cm^2 s^{-1} and source strength ~1.8 kg s^{-1}.

These parameters are consistent with release from a single central source region, followed by efficient eddy mixing (SOM-5). The central source could be activated thermally by warming of a surface zone, or by connecting subpermafrost regions to the atmosphere through seasonally opened pores in scarps or crater walls. The plume would reflect the gross morphology of active release zones (and their intensity), and the peak could suggest a region of enhanced release. For comparison, the subsolar latitude was 24°N at L_s = 122° (compare profiles b and c) and 10°N for L_s = 155° (profile d).

Additional information is obtained from a high-resolution map constructed from our data for midsummer 2003 (Fig. 3 and fig. S1). CH$_4$ appears notably enriched over several localized areas: A (east of Arabia Terra, where we also measure greatly enriched water vapor), B$_1$ (Nili Fossae), and B$_2$ (the southeast quadrant of Syrtis Major). Unusual enrichments in hydrated minerals (phyllosilicates)

The Martian methane puzzle

- Two scenarios can explain the existence of CH_4:
  - <u>Source Géophysique :</u> *dégazage depuis les couches magmatiques ou par hydrothermalisme, apport exogène (comètes, météorites)*
  - <u>Source Biologique :</u> *décomposition d'une biomasse (gaz naturel), production métabolique, i.e. VIE*

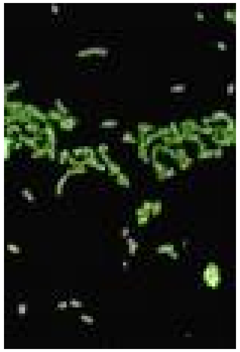

Methanogens in subsurface oceans would produce methane from their consumption of H, CO_2, etc.

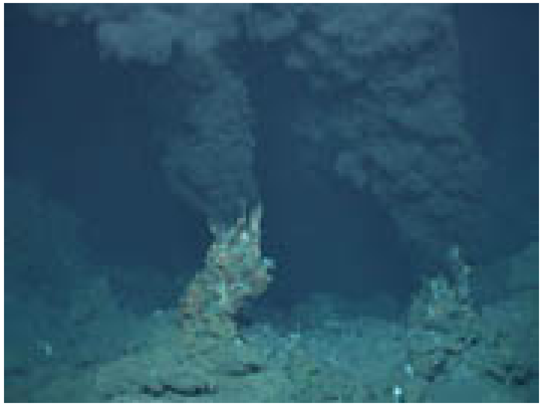

Serpentinization produces methane in undersea black smokers at Earth.

The Martian methane puzzle

- Two scenarios can explain the existence of CH4:
  - **Geophysical source :** *magmatic outgassing or hydrothermal sources*
  - Source Biologique : *décomposition d'une biomasse (gaz naturel), production métabolique, i.e. VIE*

Methanogens in subsurface oceans would produce methane from their consumption of H, CO2, etc.

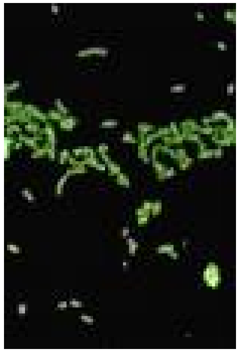

Serpentinization produces methane in undersea black smokers at Earth.

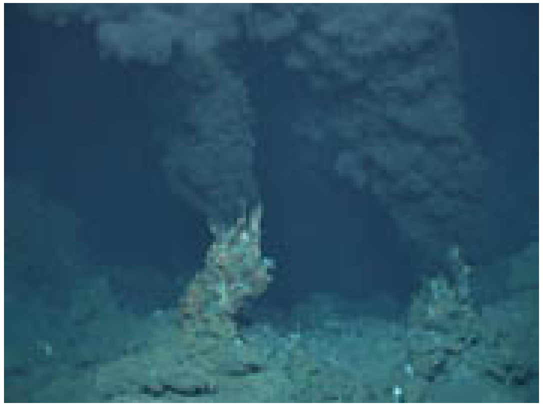

$$(Fe,Mg)_2SiO_4 + nH_2O + CO_2 \rightarrow Mg_3Si_2O_5(OH)_4 + Fe_3O_4 + CH_4$$

The Martian methane puzzle

- Two scenarios can explain the existence of CH4:
  - Source Géophysique : *dégazage depuis les couches magmatiques ou par hydrothermalisme, apport exogène (comètes, météorites)*
  - **Biological source:** *biomass decomposition (natural gas),metabolic production, i.e.* ***Life***

Methanogens in subsurface oceans would produce methane from their consumption of H, CO2, etc.

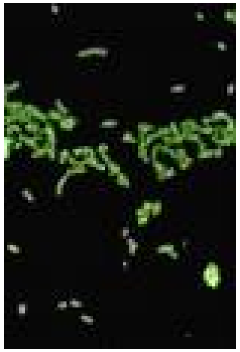

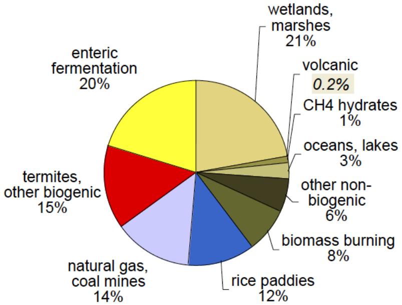

entinization
duces methane
ndersea black
kers at Earth.

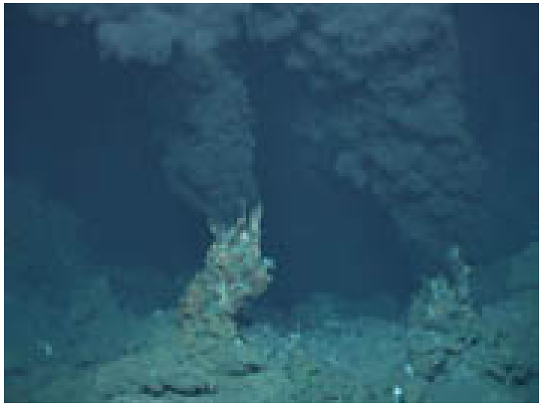

$$CO_2 + 4H_2 \rightarrow CH_4 + 2H_2O$$

However…

Mumma's observations require:

- A Methane production rate (150,000 tons emitted) comparable to the entire **Mid-Atlantic ocean ridge** (Lefèvre and Forget, 2009)
- A Methane sink term **600x stronger** than predicted by otherwise validated photochemical models (Lefèvre and Forget, 2009)
- Zahnle et al. (2011) provide lines of evidences that **Martian CH4 lie in the vicinity of terrestrial 13CH4 lines**

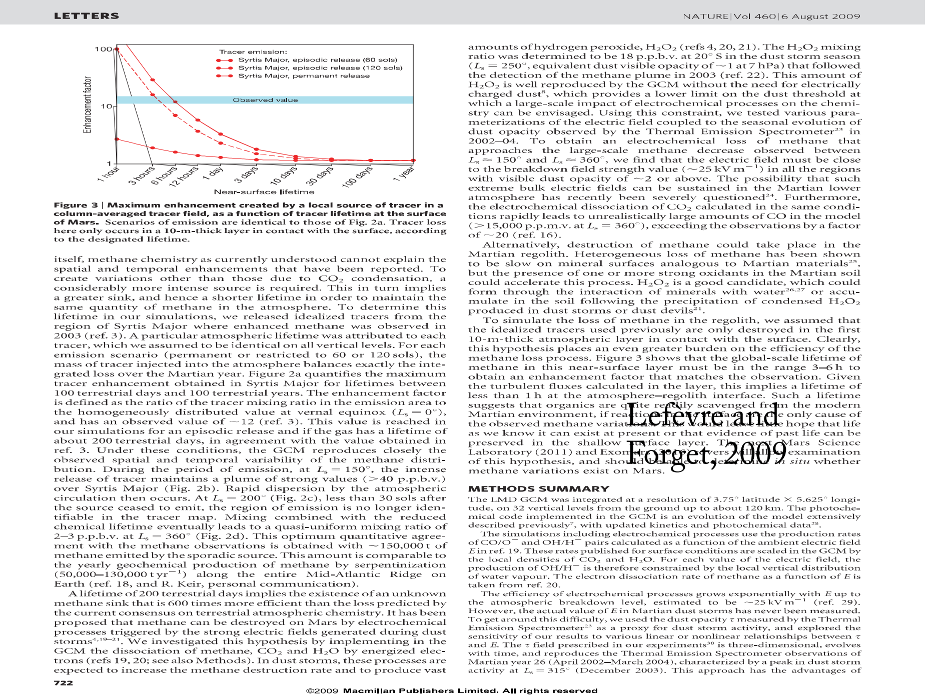

Figure 3 | Maximum enhancement created by a local source of tracer in a column-averaged tracer field, as a function of tracer lifetime at the surface of Mars. Scenarios of emission are identical to those of Fig. 2a. Tracer loss here only occurs in a 10-m-thick layer in contact with the surface, according to the designated lifetime.

itself, methane chemistry as currently understood cannot explain the spatial and temporal enhancements that have been reported. To create variations other than those due to CO_2 condensation, a considerably more intense source is required. This in turn implies a greater sink, and hence a shorter lifetime in order to maintain the same quantity of methane in the atmosphere. To determine this lifetime in our simulations, we released idealized tracers from the region of Syrtis Major where enhanced methane was observed in 2003 (ref. 3). A particular atmospheric lifetime was attributed to each tracer, which we assumed to be identical on all vertical levels. For each emission scenario (permanent or restricted to 60 or 120 sols), the mass of tracer injected into the atmosphere balances exactly the integrated loss over the Martian year. Figure 2a quantifies the maximum tracer enhancement obtained in Syrtis Major for lifetimes between 100 terrestrial days and 100 terrestrial years. The enhancement factor is defined as the ratio of the tracer mixing ratio in the emission area to the homogeneously distributed value at vernal equinox ($L_s = 0°$), and has an observed value of ~12 (ref. 3). This value is reached in our simulations for an episodic release and if the gas has a lifetime of about 200 terrestrial days, in agreement with the value obtained in ref. 3. Under these conditions, the GCM reproduces closely the observed spatial and temporal variability of the methane distribution. During the period of emission, at $L_s = 150°$, the intense release of tracer maintains a plume of strong values (>40 p.p.b.v.) over Syrtis Major (Fig. 2b). Rapid dispersion by the atmospheric circulation then occurs. At $L_s = 200°$ (Fig. 2c), less than 30 sols after the source ceased to emit, the region of emission is no longer identifiable in the tracer map. Mixing combined with the reduced chemical lifetime eventually leads to a quasi-uniform mixing ratio of 2–3 p.p.b.v. at $L_s = 360°$ (Fig. 2d). This optimum quantitative agreement with the methane observations is obtained with ~150,000 t of methane emitted by the sporadic source. This amount is comparable to the yearly geochemical production of methane by serpentinization (50,000–130,000 t yr^{-1}) along the entire Mid-Atlantic Ridge on Earth (ref. 18, and R. Keir, personal communication).

A lifetime of 200 terrestrial days implies the existence of an unknown methane sink that is 600 times more efficient than the loss predicted by the current consensus on terrestrial atmospheric chemistry. It has been proposed that methane can be destroyed on Mars by electrochemical processes triggered by the strong electric fields generated during dust storms[4,19–21]. We investigated this hypothesis by implementing in the GCM the dissociation of methane, CO_2 and H_2O by energized electrons (refs 19, 20; see also Methods). In dust storms, these processes are expected to increase the methane destruction rate and to produce vast amounts of hydrogen peroxide, H_2O_2 (refs 4, 20, 21). The H_2O_2 mixing ratio was determined to be 18 p.p.b.v. at 20° S in the dust storm season ($L_s = 250°$, equivalent dust visible opacity of ~1 at 7 hPa) that followed the detection of the methane plume in 2003 (ref. 22). This amount of H_2O_2 is well reproduced by the GCM without the need for electrically charged dust[8], which provides a lower limit on the dust threshold at which a large-scale impact of electrochemical processes on the chemistry can be envisaged. Using this constraint, we tested various parameterizations of the electric field coupled to the seasonal evolution of dust opacity observed by the Thermal Emission Spectrometer[23] in 2002–04. To obtain an electrochemical loss of methane that approaches the large-scale methane decrease observed between $L_s \approx 150°$ and $L_s \approx 360°$, we find that the electric field must be close to the breakdown field strength value (~25 kV m^{-1}) in all the regions with visible dust opacity of ~2 or above. The possibility that such extreme bulk electric fields can be sustained in the Martian lower atmosphere has recently been severely questioned[24]. Furthermore, the electrochemical dissociation of CO_2 calculated in the same conditions rapidly leads to unrealistically large amounts of CO in the model (>15,000 p.p.m.v. at $L_s = 360°$), exceeding the observations by a factor of ~20 (ref. 16).

Alternatively, destruction of methane could take place in the Martian regolith. Heterogeneous loss of methane has been shown to be slow on mineral surfaces analogous to Martian materials[25], but the presence of one or more strong oxidants in the Martian soil could accelerate this process. H_2O_2 is a good candidate, which could form through the interaction of minerals with water[26,27] or accumulate in the soil following the precipitation of condensed H_2O_2 produced in dust storms or dust devils[21].

To simulate the loss of methane in the regolith, we assumed that the idealized tracers used previously are only destroyed in the first 10-m-thick atmospheric layer in contact with the surface. Clearly, this hypothesis places an even greater burden on the efficiency of the methane loss process. Figure 3 shows that the global-scale lifetime of methane in this near-surface layer must be in the range 3–6 h to obtain an enhancement factor that matches the observation. Given the turbulent fluxes calculated in the layer, this implies a lifetime of less than 1 h at the atmosphere–regolith interface. Such a lifetime suggests that organics are quite readily scavenged from the modern Martian environment, if reactions from the surface are the only cause of the observed methane variations. This would leave little hope that life as we know it can exist at present or that evidence of past life can be preserved in the shallow surface layer. The next Mars Science Laboratory (2011) and ExoMars (2016) rovers will allow examination of this hypothesis, and should be able to determine *in situ* whether methane variations exist on Mars.

METHODS SUMMARY

The LMD GCM was integrated at a resolution of 3.75° latitude × 5.625° longitude, on 32 vertical levels from the ground up to about 120 km. The photochemical code implemented in the GCM is an evolution of the model extensively described previously[7], with updated kinetics and photochemical data[28].

The simulations including electrochemical processes use the production rates of CO/O$^-$ and OH/H$^-$ pairs calculated as a function of the ambient electric field E in ref. 19. These rates published for surface conditions are scaled in the GCM by the local densities of CO_2 and H_2O. For each value of the electric field, the production of OH/H$^-$ is therefore constrained by the local vertical distribution of water vapour. The electron dissociation rate of methane as a function of E is taken from ref. 20.

The efficiency of electrochemical processes grows exponentially with E up to the atmospheric breakdown level, estimated to be ~25 kV m^{-1} (ref. 29). However, the actual value of E in Martian dust storms has never been measured. To get around this difficulty, we used the dust opacity τ measured by the Thermal Emission Spectrometer[23] as a proxy for dust storm activity, and explored the sensitivity of our results to various linear or nonlinear relationships between τ and E. The τ field prescribed in our experiments[30] is three-dimensional, evolves with time, and reproduces the Thermal Emission Spectrometer observations of Martian year 26 (April 2002–March 2004), characterized by a peak in dust storm activity at $L_s = 315°$ (December 2003). This approach has the advantages of

Lefèvre and Forget, 2009

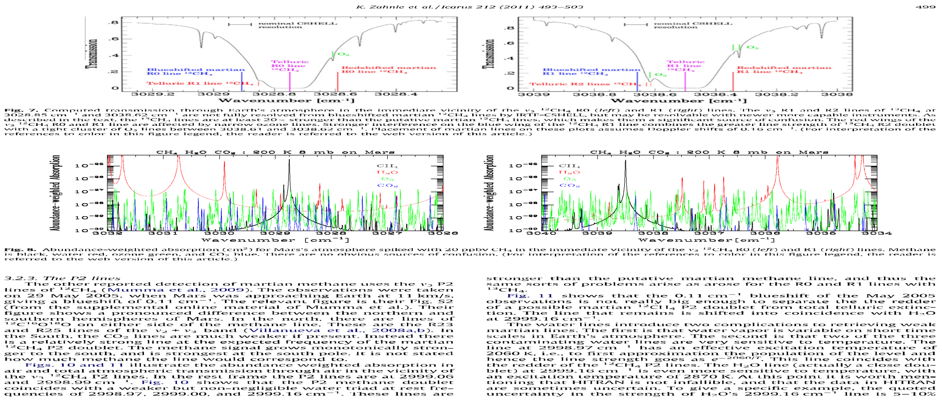

Fig. 7. Computed transmission through Earth's atmosphere in the immediate vicinity of the ν_3 $^{12}CH_4$ R0 (*left*) and R1 (*right*) lines. The ν_3 R1 and R2 lines of $^{13}CH_4$ at 3028.85 cm^{-1} and 3038.62 cm^{-1} are not fully resolved from blueshifted martian $^{12}CH_4$ lines by IRTF-CSHELL, but may be resolvable with newer more capable instruments. As described in the text, the $^{13}CH_4$ lines are at least 20× stronger than the putative martian $^{12}CH_4$ lines, which makes them a significant source of confusion. The red wings of the ν_3 $^{12}CH_4$ R0 and R1 line are affected by narrow ozone lines. Stronger interference on the blue wing of the $^{12}CH_4$ R1 line combines the greater line strength of $^{13}CH_4$ R2 doublet with a tight cluster of O_3 lines between 3038.61 and 3038.62 cm^{-1}. Placement of martian lines on these plots assumes Doppler shifts of 0.16 cm^{-1}. (For interpretation of the references to color in this figure legend, the reader is referred to the web version of this article.)

Fig. 8. Abundance-weighted absorption (cm^2) for Mars's atmosphere spiked with 20 ppbv CH_4 in the immediate vicinity of the ν_3 $^{12}CH_4$ R0 (*left*) and R1 (*right*) lines. Methane is black, water red, ozone green, and CO_2 blue. There are no obvious sources of confusion. (For interpretation of the references to color in this figure legend, the reader is referred to the web version of this article.)

3.2.3. The P2 lines

The other reported detection of martian methane uses the ν_3 P2 lines of $^{12}CH_4$ (Mumma et al., 2009). The observations were taken on 29 May 2005, when Mars was approaching Earth at 11 km/s, giving a blueshift of 0.11 cm^{-1}. The relevant figure is their Fig. S2 (from the supplemental online material of Mumma et al.). Their figure shows a pronounced difference between the northern and southern hemispheres of Mars. In the north, there are lines of $^{12}C^{16}O^{18}O$ on either side of the methane line. These are the R23 and R25 lines of the $\nu_2 + \nu_3$ band (Villanueva et al., 2008a,b). In the South, the CO_2 lines are much weaker if present. Instead there is a relatively strong line at the expected frequency of the martian $^{12}CH_4$ P2 doublet. The methane signal grows monotonically stronger to the south, and is strongest at the south pole. It is not stated how much methane the line would correspond to.

Figs. 10 and 11 illustrate the abundance weighted absorption in air and total atmospheric transmission through air in the vicinity of the ν_3 $^{12}CH_4$ P2 lines. In the rest frame the P2 lines are at 2999.06 and 2998.99 cm^{-1}. Fig. 10 shows that the P2 methane doublet coincides with a weaker but non-negligible water triad at rest frequencies of 2998.97, 2999.00, and 2999.16 cm^{-1}. These lines are stronger than the putative martian methane line, and thus the same sorts of problems arise as arose for the R0 and R1 lines with $^{13}CH_4$.

Fig. 11 shows that the 0.11 cm^{-1} blueshift of the May 2005 observations is not really big enough to separate the the redder of a possible martian $^{12}CH_4$ P2 doublet from total telluric extinction. The line that remains is shifted into coincidence with H_2O at 2999.16 cm^{-1}.

The water lines introduce two complications to retrieving weak martian lines. The first is that water vapor is variable on short time scales in Earth's atmosphere. The second is that two of the three contaminating water lines are very sensitive to temperature. The line at 2998.97 cm^{-1} has an effective excitation temperature of 2060 K, i.e., to first approximation the population of the level and hence the line strength goes as $e^{-2060/T}$. This line coincides with the redder of the $^{12}CH_4$ P2 lines. The H_2O line (actually a close doublet) at 2999.16 cm^{-1} is even more sensitive to temperature, with an excitation temperature of 2870 K. At this point it is worth mentioning that HITRAN is not infallible, and that the data in HITRAN are sometimes uncertain. To give a specific example, the quoted uncertainty in the strength of H_2O's 2999.16 cm^{-1} line is 5–10%

Zahnle et al., 2011

2011: Groundbased Observations

- Report by Mumma’s team at the Fourth International Mars atmosphere Workshop (Paris, february 2011):
  - 2009-2010 campaign
  - New instrument CRIRES: higher sensitivity and higher spectral resolution
- Results:
  - No methane detected (upper limit 1-5 ppbV)

2013: Mars Science Laboratory

SAM suite: search for organic molecules and study habitability

Atmospheric measurements:

CO_2, CO, H_2O, Ar, N_2, CH_4 (< 100 pptv)…

No detection of methane:

0 ± 1.1 ppbv

Webster et al. (Science, 2013)

2013: Mars Science Laboratory

SAM suite: search for organic molecules and study habitability

Atmospheric measurements:

CO2, CO, H2O, Ar, N2, CH4 (< 100 pptv)…

Future runs to come with 10x (at least) the current sensitivity (enrichment process)

Identifying the origin of Martian methane

Determining the origin of methane on Mars can only be addressed by looking at **methane isotopologues and at higher alkanes** (ethane, propane).

⍰ Genetic Zonation

ratio of methane/(ethane + propane) with $\delta^{13}C$ (methane)

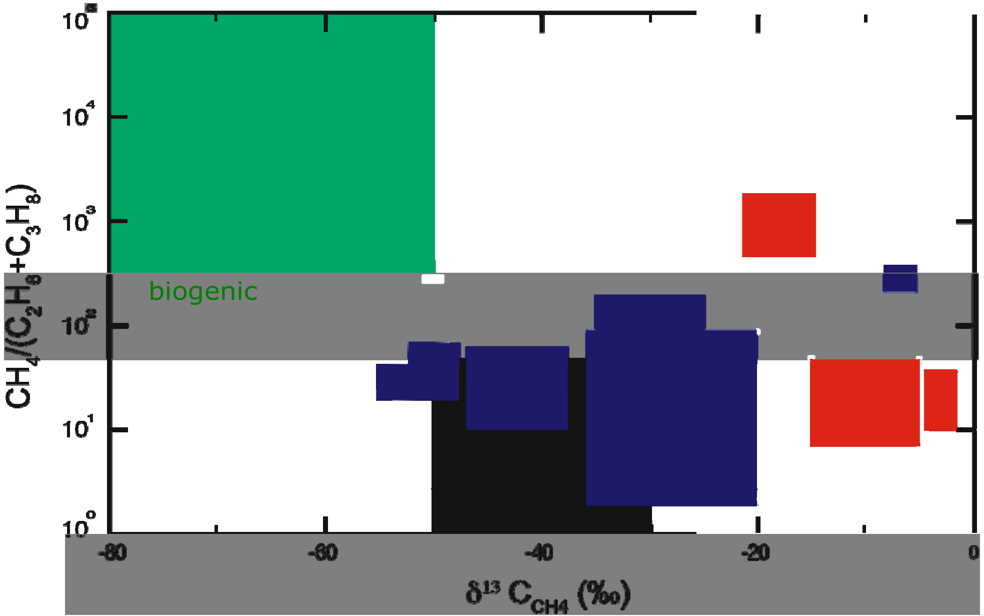

(after M. Allen/ Horita, Berndt)

[redacted]

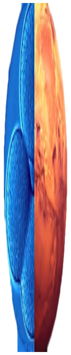

“Something that is destroyed with
a little extra precision is a
myth.”